

A Series Elastic Brake Pedal for Improving Driving Performance under Regenerative Braking

by

Umut Çalışkan

Submitted to
the Graduate School of Engineering and Natural Sciences
in partial fulfillment of
the requirements for the degree of
Master of Science

SABANCI UNIVERSITY

January, 2020

A Series Elastic Brake Pedal for Improving Driving Performance
under Regenerative Braking

Umut Çalışkan

APPROVED BY

Prof. Dr. Volkan Patođlu
(Thesis Supervisor)



Prof. Dr. Çađatay Bařdođan



Assoc. Prof. Dr. Kemalettin Erbatur



DATE OF APPROVAL: 09.12.2019

© Umut Caliskan 2020
All Rights Reserved

ABSTRACT

A SERIES ELASTIC BRAKE PEDAL FOR IMPROVING DRIVING PERFORMANCE UNDER REGENERATIVE BRAKING

UMUT ÇALIŞKAN

Mechatronics Engineering M.Sc. Thesis, 2020

Thesis Supervisor: Prof. Dr. Volkan Patoğlu

Keywords: Regenerative braking, cooperative braking, one-pedal driving, haptic pedal feel compensation, series elastic brake pedal.

Electric and hybrid vehicles are favored to decrease the carbon footprint on the planet. The electric motor in these vehicles serves a dual purpose. The use of electric motor for deceleration, by converting the kinetic energy of the vehicle into electrical energy to be stored in the battery is called *regenerative braking*. Regenerative braking is commonly employed by electrical vehicles to significantly improve energy efficiency and to help to meet emission standards.

When the regenerative and friction brakes are simultaneously activated by the driver interacting with the brake pedal, the conventional haptic brake pedal feel is disturbed due to the regenerative braking. In particular, while there exists a physical coupling between the brake pedal and the conventional friction brakes, no such physical coupling exists for the regenerative braking. As a result, no reaction forces are fed back to the brake pedal, resulting in a unilateral power flow between the driver and the vehicle. Consequently, the relationship between the brake pedal force and the vehicle deceleration is strongly influenced by the regenerative braking. This results in a unfamiliar response of the brake pedal, negatively impacting the driver's performance and posing a safety concern. The reaction forces due to regenerative braking can be fed back to the brake pedal, through actuated pedals that re-establish the bilateral power flow to recover the natural haptic pedal feel.

We propose a force-feedback brake pedal with series elastic actuation to preserve the conventional brake pedal feel during regenerative braking. The novelty of the proposed design is due to the deliberate introduction of a compliant element

between the actuator and the brake pedal whose deflections are measured to estimate interaction forces and to perform closed-loop force control. Thanks to its series elasticity, the force-feedback brake pedal can utilize robust controllers to achieve high fidelity force control, possesses favorable output impedance characteristics over the entire frequency spectrum, and can be implemented in a compact package using low-cost components.

We introduce pedal feel compensation algorithms to recover the missing regenerative brake forces on the brake pedal. The proposed algorithms are implemented for both two-pedal cooperative braking and one-pedal driving conditions. For those driving conditions, the missing pedal feedback due to the regenerative brake forces are rendered through the active pedal to recover the conventional pedal force mapping. In two-pedal cooperative braking, the regenerative braking is activated by pressing the brake pedal, while in one-pedal driving the activation takes place as soon as the throttle pedal is released.

The applicability and effectiveness of the proposed series elastic brake pedal and haptic pedal feel compensation algorithms in terms of driving safety and performance have been investigated through human subject experiments. The experiments have been conducted using a haptic pedal feel platform that consists of a SEA brake pedal, a torque-controlled dynamometer, and a throttle pedal. The dynamometer renders the pedal forces due to friction braking, while the SEA brake pedal renders the missing pedal forces due to the regenerative braking. The throttle pedal is utilized for the activation of regenerative braking in one-pedal driving. The simulator implements a vehicle pursuit task similar to the CAMP protocol and provides visual feedback to the participant.

The effectiveness of the preservation of the natural brake pedal feel has been studied under two-pedal cooperative braking and one-pedal driving scenarios. The experimental results indicate that pedal feel compensation can significantly decrease the number of hard braking instances, improving safety for both two-pedal cooperative braking and one-pedal driving. Volunteers also strongly prefer compensation, while they equally prefer and can effectively utilize both two-pedal and one-pedal driving conditions. The beneficial effects of haptic pedal feel compensation on safety is evaluated to be larger for the two-pedal cooperative braking condition, as lack of compensation results in stiffening/softening pedal feel characteristics in this case.

ÖZET

REJENERATİF FRENLEME ALTINDA SÜRÜŞ PERFORMANSINI ARTIRMAK İÇİN SERİ ELASTİK TAHRİKLİ FREN PEDALI

UMUT ÇALIŞKAN

Mekatronik Mühendisliği Yüksek Lisans Tezi, 2020

Tez Danışmanı: Prof. Dr. Volkan Patoğlu

Anahtar kelimeler: Faydalı frenleme, kooperatif frenleme, tek pedal ile sürüş, haptik pedal hissiyatı, seri elastik eyleyici tahrikli fren pedalı.

Karbon ayak izini azaltmak için elektrikli ve hibrid araçlar tercih edilmektedir. Bu araçlardaki elektrik motoru iki amaca hizmet eder. Yavaşlama için elektrik motorunun kullanılması sırasında, aracın kinetik enerjisinin aküde depolanıp elektrik enerjisine dönüştürülmesine *rejeneratif frenleme* denir. Rejeneratif frenleme, enerji verimliliğini önemli ölçüde arttırmak ve emisyon standartlarını karşılamaya yardımcı olmak için elektrikli araçlar tarafından yaygın olarak kullanılmaktadır.

Rejeneratif ve sürtünme frenleri, fren pedalıyla etkileşime giren sürücü tarafından aynı anda etkinleştirildiğinde, rejeneratif frenleme nedeniyle fren pedalı hissi bozulmaktadır. Özellikle, fren pedalı ile geleneksel sürtünme frenleri arasında fiziksel bir bağlantı olsa da, rejeneratif frenleme için böyle bir fiziksel bağlantı yoktur. Bu sebepten ötürü fren pedalına geri kuvvet beslenmez, bu da sürücü ile araç arasında tek taraflı bir güç akışı sağlar. Sonuç olarak, fren pedalı kuvveti ile aracın yavaşlaması arasındaki doğrusal olmayan ilişki ortaya çıkar. Bu bilinmeyen pedal hissiyatı, sürücünün performansını olumsuz yönde etkilemesi sürüş güvenliğini tehlikeye atmaktadır. Rejeneratif frenlemeden kaynaklanan reaksiyon kuvvetleri, alıştığımız pedal hissini geri kazanmak için ikili güç akışını yeniden kuran tahrikli pedallarla fren pedalına geri beslenebilir.

Rejeneratif frenleme sırasında geleneksel fren pedalı hissini korumak için seri elastik tahrikli, kuvvet geri beslemeli bir fren pedalı öneriyoruz. Önerilen tasarımın yeniliği, etkileşim kuvvetlerini tahmin etmek ve kapalı döngü kuvvet kontrolü yapmasıdır. Kapalı döngü kuvvet kontrolü, tahrik elemanı ile fren pedalı arasına yerleştirilen yaprak yayların deplasmanı ölçülmesiyle sağlanır. Yayların esnekliği

sayesinde, kuvvet geri beslemeli fren pedalında, yüksek doğrulukta kuvvet kontrolü elde etmek için yüksek kazançlar kullanılır. Seri elastik tahrikli fren pedalı, tüm frekans spektrumunda uygun çıkış empedans özelliklerine sahiptir ve düşük maliyetli bileşenler kullanılarak kompakt bir dizayn şeklinde araçlara konulabilir.

Fren pedalındaki eksik rejeneratif fren kuvvetlerini geri kazanmak için pedal hissiyatı telafi algoritmaları sunuyoruz. Önerilen algoritmalar, hem iki pedallı kooperatif frenleme hem de tek pedallı sürüş için uygulanmıştır. Bu sürüş koşulları için, rejeneratif fren kuvvetlerine bağlı eksik pedal kuvvetinin geri verilmesi, telafi edilmiş rejeneratif fren kuvvetleri ve telafi edilmemiş fren kuvvetleri olarak incelenir. İki pedallı kooperatif frenlemede, rejeneratif frenleme fren pedalına basılarak etkinleştirilirken, tek pedallı sürüşte, gaz pedalı bırakıldığında aktivasyon gerçekleşir.

Önerilen seri elastik fren pedalı ve haptik pedal hissi algoritmalarının, sürüş güvenliği ve performansı açısından etkinliği insanlı deneyler ile araştırılmıştır. Deneyler, seri elastik tahrikli fren pedalı, tork kontrollü bir dinamometre ve bir gaz pedalından oluşan haptik pedal hissetme platformu kullanılarak gerçekleştirilmiştir. Sürtünme freninden kaynaklanan pedal kuvvetleri dinamometre tarafından benzetilir. Seri elastik tahrikli fren pedalı rejeneratif frenleme nedeniyle eksik pedal kuvvetlerini insan ayağına geri besler. Gaz pedalı, tek pedallı sürüşte rejeneratif frenlemenin etkinleştirilmesi için kullanılır. Simülatör, CAMP protokolüne benzer bir araç takip görevi yürütür ve katılımcıya görsel geri bildirim sağlar.

İnsanlı deneylerin sonucunda, pedal hissi telafisinin sert frenleme sayısını önemli ölçüde azalttığı ve hem iki pedallı kooperatif frenleme hem de tek pedallı sürüş güvenliğini arttırdığı gözlemlenmiştir. Yapılan anketlerin sonucuna göre, hem iki pedallı hem de tek pedallı sürüş koşullarını eşit şekilde tercih edilmiştir. Gönüllüler pedal hissi telafisini güçlü bir şekilde tercih etmişlerdir. Haptik pedal hissi telafisinin güvenlik üzerindeki yararlı etkilerinin, iki pedallı kooperatif frenleme koşulu için daha büyük olduğu görülmüştür, çünkü bu durumda telafi eksikliği, pedalın sertleşme / yumuşama hissiyatı daha büyük olur.

« *To my beloved family and wife* »

ACKNOWLEDGEMENTS

It is a great pleasure to work under the supervision of Prof. Dr. Volkan Patođlu. His guidance, wisdom, and support during my master's are priceless. Thanks to his vision, I fell in love with research in the robotic field.

I would gratefully thank Assoc. Prof. Dr. Kemalettin Erbatur and Prof. Dr. ađatay Bařdođan for spending their valuable time to serve as my jurors. I would like to thank Assoc. Prof. Dr. Kemalettin Erbatur for humbleness and understanding during my teaching assistant. I admire his work ethic and passion for his work.

I would like to thank my fellow lab members; Gökhan Alcan for his advice and helpfulness, Mehmet Emim Mumcuođlu, Naida Fetic, Emre Yılmaz for his kindness and for sharing memorable moments, Vahid Tavakol and Arda Ađbabaođlu for his ideas, creativity, and support.

I would like to thank Mustafa Yalın, Gokay oruhlu, İlker Sevgen, and Zafer ömleki for their great help on my research. I have successfully overcome the obstacles during my research with their great experience in their respective fields.

I would like to thank the HMI group, Burak Öztoprak, ađatay Irmak, Batuhan Toker, Cansu Öztürk, Mahmut Beyaz, Ali Yařar, Ayhan Yılmaz, Uđur Mengilli, Fatih Emre Tosun, Özge Orhan, and Ali Khalilian Motamed Bonab for their comradeship. I am grateful for Fatih Emre Tosun's companionship during my master's study. I am wishing all the best in his Ph.D. career. I am greatly thankful to Ali Khalilian Motamed Bonab, Uđur Mengilli and Özge Orhan for their support and their friendship during endless and countless hours working together. They are a great inspiration for me in terms of work ethic, knowledge and dedication to research. I wish them a very bright future.

I would like to thank my precious parents Salim and Mine for their invaluable love and never-ending support from the beginning of my life. I am grateful to Elin Güner for her kindness and priceless her love.

Finally, I would like to thank my beloved wife İlayda for her endless love, encouragement and support throughout my sleepless nights.

Contents

| | |
|-----------------------------|-------------|
| Abstract | iii |
| Özet | v |
| Acknowledgements | viii |
| Contents | ix |
| List of Figures | xiii |
| List of Tables | xv |
| Nomenclature | xvi |
| 1 Introduction | 1 |
| 1.1 Motivation | 1 |
| 1.2 Contributions | 5 |
| 1.3 Outline | 7 |

| | | |
|----------|---|-----------|
| 2 | Related Work | 8 |
| 2.1 | Regenerative Braking for Electric and Hybrid Vehicles | 8 |
| 2.1.1 | Two-Pedal Driving | 8 |
| 2.1.2 | One-Pedal Driving | 10 |
| 2.2 | Brake-by-Wire Systems | 10 |
| 2.3 | Pedal Feel Compensation Devices for Regenerative Braking | 11 |
| 2.3.1 | Passive Approaches | 11 |
| 2.3.2 | Active Approaches for Compensating Missing Regenerative Braking Forces | 12 |
| 2.3.2.1 | Electrohydraulic Approaches | 12 |
| 2.3.2.2 | Electromechanic Approaches | 13 |
| 2.4 | Series Elastic Brake Pedal | 14 |
| 3 | Design and Control of Series Elastic Brake Pedal | 15 |
| 3.1 | Mechanical Design | 17 |
| 3.2 | Sensors and Power Electronics | 19 |
| 3.3 | Cascaded Loop Controller for SEA Brake Pedal | 20 |
| 4 | Design and Control of Haptic Pedal Feel Rendering Platform | 22 |
| 4.1 | Mechanical Design of Haptic Pedal Feel Rendering Platform | 22 |
| 4.1.1 | Throttle Pedal | 23 |
| 4.2 | Control of the Haptic Pedal Feel Rendering Platform | 23 |
| 5 | Experimental Characterization of SEA Brake Pedal | 26 |
| 5.1 | System Identification | 26 |
| 5.2 | Force Bandwidth | 28 |

| | | |
|----------|---|-----------|
| 5.3 | Force Tracking Performance | 30 |
| 6 | Haptic Pedal Feel Compensation Algorithms | 32 |
| 6.1 | Conventional Haptic Brake Pedal Feel | 33 |
| 6.2 | Brake Force Generator | 33 |
| 6.2.1 | Brake Pedal Displacement to Deceleration Mapping | 34 |
| 6.2.2 | Brake Force Distribution | 34 |
| 6.2.3 | Brake Pedal Force Mapping | 35 |
| 6.3 | Two-pedal Cooperative Braking and One-pedal Driving Simulations | 35 |
| 6.3.1 | Two-Pedal Cooperative Braking | 37 |
| 6.3.2 | One-Pedal Driving | 37 |
| 7 | User Evaluations | 40 |
| 7.1 | Participants | 40 |
| 7.2 | Driving Simulator | 40 |
| 7.3 | Task | 41 |
| 7.4 | Experimental Procedure | 42 |
| 7.5 | Performance Metrics | 42 |
| 7.6 | Analysis | 43 |
| 7.7 | Experiment Results | 43 |
| 7.7.1 | Safety | 43 |
| 7.7.2 | Pursuit Tracking Performance | 44 |
| 7.7.3 | Energy Efficiency | 44 |
| 7.7.4 | Qualitative Metrics | 45 |
| 8 | Discussion of User Studies | 50 |

9 Conclusion

54

Bibliography

55

List of Figures

| | | |
|-----|--|----|
| 1.1 | Regenerative and friction brake forces | 2 |
| 1.2 | Block diagram of cooperative regenerative braking | 3 |
| 3.1 | SEA brake pedal prototype | 17 |
| 3.2 | Mechatronic design of the SEA brake pedal and the dynamometer . | 18 |
| 3.3 | Deflection of leaf spring in cross-flexure joint | 19 |
| 3.4 | Measuring the deflection of cross-flexure joint by linear encoder . . | 20 |
| 3.5 | Block diagram of SEA brake pedal | 21 |
| 4.1 | Regenerative brake development platform consists of a force-feedback brake pedal and a torque controlled test dynamometer | 23 |
| 4.2 | Control block diagram of haptic pedal feel rendering platform . . . | 24 |
| 4.3 | Haptic pedal feel rendering platform for cooperative braking | 25 |
| 5.1 | Closed-loop system used for identification of the SEA brake pedal . | 27 |
| 5.2 | Experimental system identification of the SEA brake pedal | 28 |
| 5.3 | Low force (5 Nm) bandwidth, medium force (10 Nm) bandwidth, high force (15 Nm) bandwidth | 29 |
| 5.4 | Step input force tracking performance in 10 [Nm] | 30 |
| 5.5 | Chirp input force tracking performance in 10 [Nm] | 31 |

| | | |
|-----|---|----|
| 6.1 | Control block diagram of haptic pedal feel rendering platform . . . | 33 |
| 6.2 | A sample scenario for two-pedal cooperative braking with and without haptic pedal feel compensation | 36 |
| 6.3 | A sample scenario for one-pedal driving with and without haptic pedal feel compensation | 38 |
| 7.1 | Cooperative braking simulator | 41 |
| 7.2 | Box plot of number of hard brakings | 47 |
| 7.3 | Box plot of percent throttle use | 48 |
| 7.4 | Box plot of regenerative braking energy | 48 |
| 7.5 | Sample experimental results collected under uncompensated and compensated conditions | 49 |

List of Tables

| | | |
|-----|---|----|
| 5.1 | SEA brake pedal plant parameters and controller gains | 28 |
| 7.1 | Survey Questions and Summary Statistics | 45 |

Nomenclature

| | |
|--------------|--|
| m | Mass of the brake pedal |
| b | Damping of the brake pedal |
| K | Stiffness of the series elastic element |
| P_m | Proportional motion controller gain |
| I_m | Integral motion controller gain |
| P_f | Proportional force controller gain |
| F_{fric}^b | Desired dynamometer force |
| F_{reg}^b | Desired SEA brake pedal force |
| F_m | Applied motor torque |
| v_m | Measured motor velocity |
| F_h | Human force |
| F_h^* | Feedthrough human leg force |
| F_{hyd} | Dynamometer force applied into brake pedal |
| F_{SEA} | SEA brake pedal force |
| x_{brake} | Brake pedal position |
| x_{gas} | Gas pedal position |
| a_{car}^d | Desired vehicle deceleration |
| v_{car}^d | Velocity of the vehicle |
| F_{fric}^d | Desired friction brake force |
| F_{reg}^d | Desired regenerative brake force |
| F_{fric} | Actual friction brake force |
| F_{reg} | Actual regenerative brake force |

Chapter 1

Introduction

1.1 Motivation

With the current emphasis on decreasing smog forming emissions, electric and hybrid vehicles are becoming ubiquitous. The electric motors on these vehicles assume dual purpose. Not only can they be used to accelerate the vehicle, but they can also be employed as generators to decelerate the vehicle. The use of electric motor for deceleration, by converting the kinetic energy of the vehicle into electrical energy to be stored in the battery, is called regenerative braking. Regenerative braking is crucial as it can significantly improve the range of the vehicle by improving its energy efficiency. Along these lines, it is desirable to employ regenerative braking as much as possible, while decelerating the vehicle.

Regenerative braking is commonly employed by electrical and hybrid vehicles in order to significantly improve their energy efficiency and help them meet emission standards [1]. In these vehicles, whenever deceleration is demanded, regenerative braking uses the electric motor of the vehicle as a generator to convert its kinetic energy into electrical energy to charge the battery pack, instead of dissipating that energy through heat as in conventional friction braking. While regenerative braking is crucial for power efficiency, its utilization is challenging since the regenerative braking force is a nonlinear function of the vehicle speed and constrained by the

size of the electrical motor as well as the amount of charge that the battery pack can accept at any given instant. For instance, in general, regenerative braking cannot be applied at low and high speed regions; sufficient braking forces cannot be generated at low speeds, while batteries cannot be charged at high speeds without causing permanent damage. Consequently, conventional friction brakes are still required to be employed together with regenerative braking to achieve safe deceleration [2].

Figure 1.1 presents a sample cooperative regenerative braking scenario, where initially the vehicle is moving at 50 km/h. At $t=1$ sec, the driver presses the brake pedal, linearly increasing its displacement to a certain level, and keeps it constant until the vehicle stops. The third row of the figure depicts the demanded brake force (mapped from the pedal displacement), along with the contributions from the regenerative braking and the friction braking. In this figure, one can observe that initially only the regenerative braking is used, but at around $t = 1.2$ s, the brake

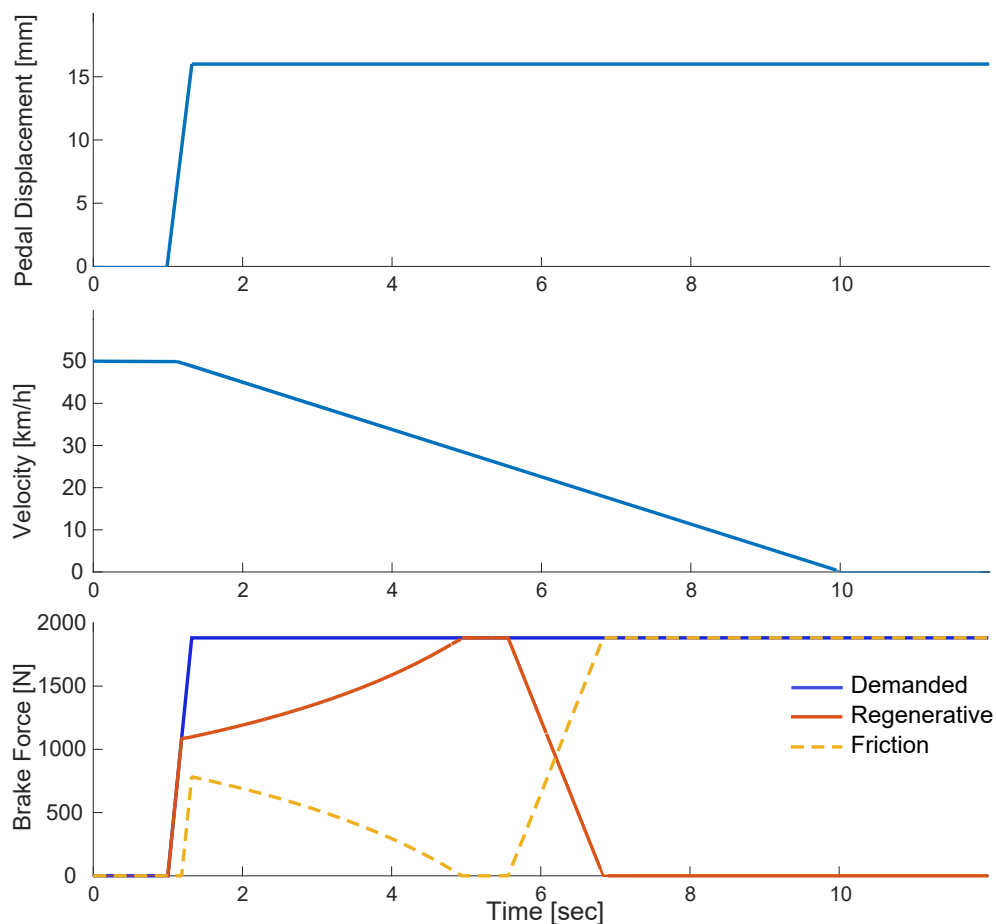


FIGURE 1.1: Regenerative and friction brake forces

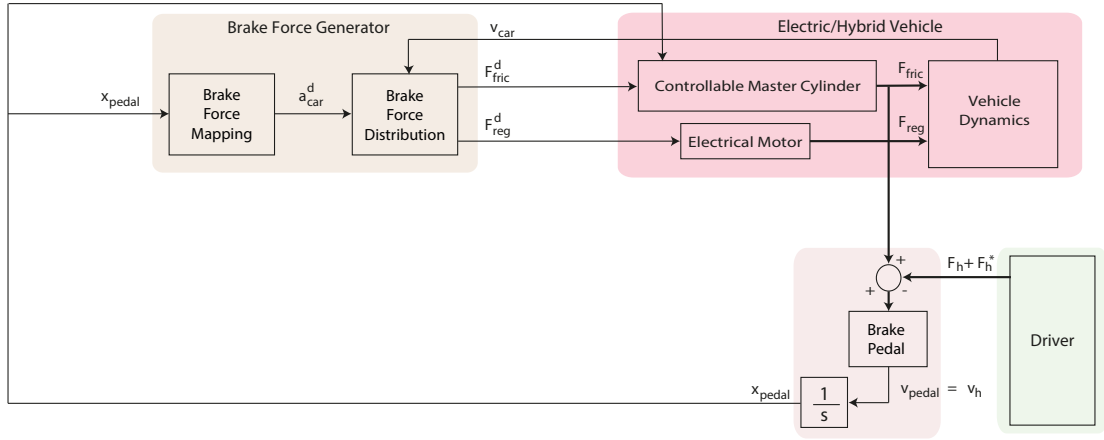


FIGURE 1.2: Block diagram of cooperative regenerative braking

force demand exceeds the amount that can be supplied by the regenerative braking at that particular speed and charge level; hence, the friction brakes are employed. As the vehicle slows down, the regenerative braking capacity increases, until a speed threshold after which no regenerative brake force can be generated. To ensure the constant brake demand is provided, the friction brake is first decreased and then increased accordingly. The friction brake forces are modulated by varying the mapping between the pedal displacement and the master cylinder [3–5].

Figure 1.2 presents the block diagram for cooperative regenerative braking. Thick lines denote mechanical coupling, while thin lines represent signals. In this diagram, the pedal displacement is continually measured and mapped to the desired deceleration. Given the desired vehicle deceleration, the brake force distribution block considers the instantaneous regenerative braking capacity, as well as road the conditions to generate the brake force references for both the regenerative and the friction braking systems. Even though both the regenerative and the friction brake forces act on the vehicle to slow it down, there exists a physical connection between the brake pedal and the friction brakes, while no such connection exists for the regenerative braking. Along these lines, only the reaction forces from the friction brakes are fed back to the user. Note that, without any compensation, these reaction forces will result in an unnatural and unconventional brake feel.

In particular, for the scenario in Figure 1.1, for a constant pedal displacement, the brake pedal will first feel stiff around $t = 1.2$ s, then suddenly become compliant

after $t = 1.5$ s, and then feel stiff again after $t=5.5$ s. Such sudden changes in pedal feel is undesirable, as this nonlinear relationship that depends on the vehicle state is very hard to learn, making it challenging to control vehicle deceleration.

Abrupt pedal feeling under regenerative braking should be compensated by an additional actuator to ensure safe deceleration. An additional actuator's main purpose is to recover the missing regenerative braking forces. In particular, electro-hydraulic brake pedal actuators are used in the vehicle industry for regulating the pressure of the hydraulic fluid. Electromechanical solutions are proposed to recover the missing regenerative brake forces. Moreover, these solutions can be utilized in brake by wire systems in the future. Another solution for the regenerative braking and friction braking blending algorithm named one-pedal driving. This solution enables to activate regenerative brake when releasing the gas pedal. The brake pedal is just for friction braking. Thus, an unconventional brake feel is not felt by the driver.

1.2 Contributions

In this thesis, we proposed an active brake pedal with force feedback and algorithms to compensate for the pedal feel in electric vehicles, under two-pedal cooperative braking and one-pedal driving. The force-feedback brake pedal is implemented as a single degree-of-freedom device with a series elastic actuation (SEA) [6]. Additionally, a haptic test platform is introduced for evaluation of the pedal feel compensation algorithms in a number of simulated vehicle pursuit tasks. The test platform consists of the SEA brake pedal, the torque control dynamometer and the throttle pedal. The effectiveness of the preservation of the natural brake pedal feel has been studied under two-pedal cooperative braking and one-pedal driving scenarios.

The contributions of this thesis can be summarized as follows:

- We present the design and control of a series of elastic brake pedal. SEA brake pedal trades off force-control bandwidth for force control fidelity and improved coupled stability, by introducing a compliant force sensing element into the closed-loop force control [7]. By decreasing the force sensor stiffness, it allows higher force controller gains to be utilized for robust force-controllers, without sacrificing stability. SEA can effectively mask the inertia of the actuator side from the interaction port, featuring favorable output impedance that is safe for human interaction over the entire frequency spectrum. Furthermore, SEA brake pedal can be implemented at a significantly lower cost than traditional force sensor based implementations.
- We introduce a torque-controlled dynamometer to render (electro)hydraulic friction brake reaction forces originating from the vehicle's controllable master cylinder, as well as other forces/disturbances acting on the brake pedal. The dynamometer shares the identical design with the SEA brake pedal, but has an independent controller. There exists a physical connection between the dynamometer and the SEA brake pedal, similar to that of a conventional brake pedal and a master cylinder.

-
- We present pedal feel compensation algorithms for one-pedal driving and two-pedal driving to blend regenerative braking and friction braking. In one-pedal driving, the regenerative brake is activated by releasing the throttle pedal and the brake pedal is used for additional friction braking. On the contrary, regenerative braking and friction braking are activated by the brake pedal during two-pedal driving.
 - We propose a driving simulator to evaluate the efficacy of one-pedal driving and two-pedal driving condition. The simulator provides visual feedback to the driver and contains a haptic pedal feel platform for rendering pedal forces. Compensated two-pedal driving, uncompensated two-pedal driving, compensated one-pedal driving, and uncompensated one-pedal driving are evaluated in terms of driver safety, energy efficiency, and driving performance in the braking simulator. The simulator implements a vehicle pursuit task according to the Crash Avoidance Metrics Partnership (CAMP) protocol.
 - We provide evidence that compensation of regenerative braking forces leads to safer and better driving experience. In particular, the number of hard brakings in compensated two-pedal cooperative braking and compensated one-pedal driving are shown to be statistically significantly less than uncompensated conditions. Furthermore, energy recovery in one-pedal driving is statistically significantly higher compared to the two-pedal cooperative braking condition, while throttle use is statistically significantly less in the two-pedal cooperative braking condition. Overall, it is shown that the one-pedal driving and two-pedal cooperative braking are both viable options for electric vehicles, but a force-feedback pedal is highly recommended for the compensation of the missing regenerative braking forces in both driving conditions.

1.3 Outline

The rest of the thesis is organized as follows:

Chapter 2 provides related works on about pedal feel compensation devices and braking algorithms.

Chapter 3 presents the mechanical and control design of the SEA brake pedal.

Chapter 4 provides the mechatronics design and implementation details of the SEA brake pedal, the dynamometer, and the throttle pedal.

Chapter 5 presents the experimental characterization of the SEA brake pedal and provides force control bandwidth, motion control bandwidth, and force tracking the performance of the system.

Chapter 6 introduces the algorithms that are implemented for compensating pedal feel under regenerative braking and for the distribution of brake forces in one-pedal driving and two-pedal cooperative braking.

Chapter 7 provides the experimental procedure for human subject experiments under the two-pedal cooperative braking and one-pedal driving conditions, conducted to evaluate the efficacy of SEA brake pedal and comparison algorithms with the haptic pedal feel platform.

Chapter 8 provides an overview of the efficacy of the SEA brake pedal and the evaluation of the driving algorithms.

Chapter 9 concludes the thesis and discusses future research directions.

Chapter 2

Related Work

In this chapter, a literature review is presented for methods and devices that provide more conventional brake pedal feel under regenerative braking. Blending algorithms for regenerative braking and friction braking have also been reviewed.

2.1 Regenerative Braking for Electric and Hybrid Vehicles

In this section, two distinct approaches to employ regenerative braking in vehicles are presented as two-pedal and one-pedal driving conditions.

2.1.1 Two-Pedal Driving

Parallel and *cooperative* regenerative braking [5, 8] rely on brake pedal position to employ regenerative braking. For that reason, they are categorized as *two-pedal driving* braking algorithms. During parallel braking, conventional friction brakes are always in use, while regenerative braking is used to augment them when there is demand for further deceleration and sufficient regenerative braking force is available. Parallel braking only requires the control of additional regenerative

brake while friction brakes are operated directly via the brake pedal displacement. While parallel braking is relatively easier to implement, this approach lacks power efficiency due to its generous use of friction brakes.

Cooperative braking is a commonly used approach to blend regenerative and friction braking. In cooperative braking, when the brake pedal is pressed, the regenerative braking is utilized as much as possible to provide the demanded deceleration, while simultaneously charging the battery pack. The friction brakes are activated minimally, only to supplement regenerative braking, when the deceleration demand is higher than what can be provided solely by the regenerative braking [5, 8]. In the literature, it has been shown that cooperative braking can be very efficient and recover up to 50% more energy compared to alternative regenerative braking approaches [4, 5].

In two-pedal cooperative braking, when the regenerative and friction brakes are simultaneously activated by the driver interacting with the (emergency) brake pedal, the conventional haptic brake pedal feel is disturbed due to regenerative braking. In particular, while there exists a physical coupling between the brake pedal and the conventional (electro)hydraulic friction brakes, no such physical coupling exists for the regenerative braking. As a result, no reaction forces are fed back to the brake pedal, resulting in a unilateral power flow between the driver and the vehicle. Consequently, the relationship between the brake pedal force and the vehicle deceleration is strongly influenced by the regenerative braking. When regenerative/friction braking is activated/deactivated, the pedal response may change abruptly, resulting in rapid softening/stiffening of the brake pedal. This unfamiliar response of the brake pedal poses a safety concern, since it may negatively impact the driver performance.

Reaction forces due to regenerative braking can be fed back to the brake pedal, through actuated pedals that re-establish the bilateral power flow between the brake pedal and the vehicle to recover the natural haptic pedal feel. Along these lines, electro-hydraulic [3–5] and electro-mechanical [9, 10] force-feedback brake pedals have been proposed in the literature.

2.1.2 One-Pedal Driving

One-pedal driving utilizes regenerative braking based on the position of throttle pedal. When driver releases the accelerator pedal, a predetermined regenerative brake force is applied by the electric motor [11, 12]. One-pedal driving may reduce the reaction time of the drivers while braking [13]. One-pedal driving may also simplify the driving experience, by operating just one-pedal to drive the vehicle [14].

However, deceleration rate that can be achieved with regenerative braking has limitations. In addition to the limitations, for maintaining the driving comfort, adequate deceleration rate should be selected for regenerative braking. Thus, friction brakes are still required for emergency situations or higher deceleration rates which are beyond regenerative brake. Besides, the regulations mandate a physical connection between brake pedal and brake pads.

Friction braking and regenerative braking are utilized together to achieve safe deceleration. When the driver requires a larger brake force than the predetermined or maximum capacity of the regenerative brake force, the driver employs the friction braking by pressing the brake pedal. During these interactions, the regenerative brake force may diminish at the critical velocities or due to limitations of regenerative braking, the driver cannot feel the force difference in the brake pedal. This may lead to abrupt driving experience and uncertain braking distances for the driver. Therefore, recovery of missing reaction forces regenerative brake is an important sensory feedback during braking.

2.2 Brake-by-Wire Systems

Several approaches have been proposed to achieve a smooth conventional brake pedal feel for cooperative regenerative brake systems. One approach is to decouple mechanical connection between the brake pedal and the brake pads, to result in a brake-by-wire system [15]. In this approach, pedal displacement is measured and

required friction brake forces are applied through remote actuators without any force coupling with the brake pedal. Consequently, the pedal feel is not affected by the mechanical connection between the brake pads and the brake pedal.

Brake-by-wire systems is employed to the rear brakes of F1 cars to reduce the overall weight. While brake-by-wire systems hold great promise, currently they are not widely used, as a mechanical coupling between the friction brakes and the brake pedal is demanded by safety regulations.

2.3 Pedal Feel Compensation Devices for Regenerative Braking

In this section, we evaluate the current approaches to compensate for the missing regenerative forces. In general, an additional device for display the brake pedal forces to the driver is required. Similarly, if the brake by wire systems are implemented in vehicles, force-feedback with an electromechanical infrastructure is likely to have an edge compared to electrohydraulic systems.

2.3.1 Passive Approaches

Passive approaches provide pedal feel by utilizing various elastic and dissipation elements to implement pre-determined force-displacement relationship for the brake pedal [16, 17]. In [18], adjustable damping is implemented with magnetorheological fluids. While passive approaches are low-cost and simple, they can only be used for brake-by-wire systems, as they lack active force rendering capability or online adjustability to recover conventional brake feel when friction brake forces are reflected back to the driver through a physical connection.

2.3.2 Active Approaches for Compensating Missing Regenerative Braking Forces

Active approaches provide pedal forces to the driver through an actuator. Active approaches can be loosely categorized as *electromechanic devices* and *electrohydraulic devices*.

2.3.2.1 Electrohydraulic Approaches

Since hydraulic friction brakes are widespread in the automotive industry, electrohydraulic systems have also been adapted to work with regenerative braking [3–5, 19, 20]. In particular, a standard hydraulic friction brake system needs to be modified such that the mapping between the brake pedal displacements and the friction brake forces becomes continually adjustable to match the requirements of cooperative regenerative braking. Along these lines, in [5], a linear solenoid actuator has been introduced between the master cylinder and the brake pedal to control the gap between them. In [3], multiple pumps and controlled valves are orchestrated through an electronic stability program modulator to achieve cooperative regenerative braking. The system in [4] relies on a servo controlled master cylinder together with a tandem motor cylinder to control the brake forces given a brake pedal displacement. While such modifications can ensure a good mapping between the pedal displacement and the total braking force, they do not address the problem of the brake pedal feel. In [4], a separate hydraulic brake pedal feel simulator is added to the system to recover conventional brake feel. Similar electrohydraulic and electromechanical-hydraulic solutions have been proposed in [19, 20].

Conventional friction brakes are commonly implemented using (electro)hydraulics. When the brake pedal is pressed, hydraulic fluid is pushed into the master cylinder where the hydraulic forces are multiplied by a brake booster and sent to the activate the brake pads. Consequently, the brake pads apply longitudinal forces to the discs to create friction between the discs and the brake pads. Thanks to the hydraulic fluid, there exists a physical power exchange between the brake pedal

and the friction brakes, and whenever a driver pushes the pedal, she/he feels the reaction forces due to this physical coupling.

2.3.2.2 Electromechanic Approaches

Active approaches provide pedal forces through an actuated pedal. For instance in [9], a geared electric motor is used to impose the motion of the brake pedal under closed-loop control based on measurements from the pedal. In this implementation, spring can also be connected in parallel to the electric actuator to supplement it with spring forces. Since the structure is motion-controlled, it is not suitable for physical human-robot interaction (pHRI). In [21], an active brake pedal simulator is introduced to achieve the desired brake feel through closed-loop force control. In particular, a torque sensor and a geared DC motor are employed for explicit force control of the brake pedal. The high stiffness of the force sensor limits the closed-loop gain due to the fundamental limitations of force control. This may lead to poor driver performance. In [22], a brake simulator is proposed where resistive forces are applied by selectively immobilizing the base of a spring. In [23], a reaction force observer is used together with motor current feedback to control the pedal force with a geared actuator. Disturbances and the human forces cannot be separated in reaction torque observer. Thus, the system requires a frictionless design. In related studies, haptic interfaces are proposed to provide force-feedback to accelerator pedals based on open-loop torque control of direct-drive and capstan-driven actuators [10, 24]. A very large motor is required to supply enough brake pedal force to the driver in the direct-drive systems for the brake pedal applications.

2.4 Series Elastic Brake Pedal

SEA brake pedal trades off force-control bandwidth for force control fidelity and improved coupled stability, by introducing a compliant force sensing element into the closed-loop force control [7]. By decreasing the force sensor stiffness, it allows higher force controller gains to be utilized for robust force-controllers, without sacrificing stability. SEA can effectively mask the inertia of the actuator side from the interaction port, featuring favorable output impedance that is safe for human interaction over the entire frequency spectrum. Furthermore, SEA brake pedal can be implemented at a significantly lower cost than traditional force sensor based implementations.

Chapter 3

Design and Control of Series Elastic Brake Pedal

In this chapter, an active force-feedback brake pedal is proposed to preserve conventional pedal feel under regenerative braking. The active force-feedback brake pedal is implemented as a single degree of freedom force-feedback device with series elastic actuation (SEA) [6]. The novelty of the proposed design is due to the deliberate introduction of a compliant element between the actuator and the brake pedal, whose deflections are measured to estimate interaction forces and to perform closed-loop force control. By using compliant force sensing elements in the explicit force control framework, SEA enables higher force-feedback controller gains to be utilized to achieve responsive and robust force-control.

SEA brake pedal also possesses favorable output impedance characteristics over the entire frequency spectrum. In particular, within the force control bandwidth of the device, SEA can ensure high fidelity force rendering and backdrivability through active force control, that is, by modulating its output impedance to desired level. For the frequencies over the control bandwidth, the apparent impedance of the system is limited by the inherent compliance of the force sensing element, that acts as a physical filter against impulsive loads and high frequency disturbances (e.g., vibrations originating from ABS) [25].

Compared to load cell or other commercial force sensor based control approaches, SEA brake pedal employs an orders of magnitude more compliant force sensing element. Under the action of interaction forces, this compliant sensor experiences large deflections that can be measured using regular position sensors, such as optical encoders or hall effect sensors. Consequently, robust and low-cost force sensors can be implemented based on regular position sensing and custom built compliant springs.

Furthermore, since the use of compliant force sensor enables larger control gains to be used without sacrificing the inherent stability limits imposed due to sensor-actuator non-collocation [26], the force controller becomes more robust against disturbances and unmodelled dynamics. Along these lines, lower cost components can be utilized as actuators/power transmission elements in the implementation of a SEA brake pedal. Revoking the need for high precision and inevitably expensive load cells, actuators and transmission elements, SEA brake pedal can be built in a compact package at a significantly lower cost [27].

SEA trades-off force-control bandwidth for fidelity: a significant increase of the sensor compliance results in a relatively low closed-loop control bandwidth [28]. Luckily, given the relatively low bandwidth of human movements, an appropriate stiffness of the compliant element can be determined such that the SEA brake pedal can respond fast enough to match the requirements of the braking task.

Thanks to its high-fidelity force control performance, SEA brake pedal not only can be used to compensate for the parasitic effects of regenerative braking on the pedal feel, but also can provide adjustable brake pedal feel for different vehicle settings in electrical and hybrid vehicles. In particular, pedal force feedback can be adjusted to match different vehicle modes (e.g., sport or comfort), as commonly implemented for steering, throttle and suspension responses. SEA brake pedal prototype is depicted in Figure 3.1.



FIGURE 3.1: SEA brake pedal prototype

3.1 Mechanical Design

The main actuation mechanism and dimensions of the SEA brake pedal have been designed to be compatible with existing brake pedals, such that SEA brake pedal can be connected to existing friction brakes in parallel with minimal modifications. For power transmission, a geared DC motor with large torque output capacity is used to drive a capstan transmission. The capstan transmission consists of a pinion attached to the geared motor and a driven sector pulley. In particular, the capstan transmission not only helps improve the torque output, but also embeds the intentionally introduced compliant joint element and a position sensor to measure deflections of this compliant element.

The brake pedal is attached to the vehicle frame through a ball-bearing, and the sector pulley is attached to the brake pedal through a cross-flexure pivot. A cross-flexure pivot is a robust and simple *compliant* revolute joint with a large range of

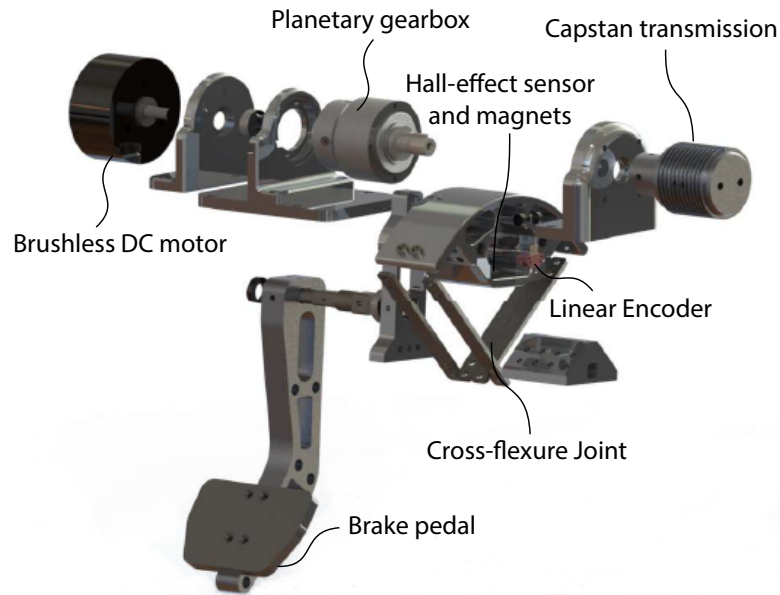


FIGURE 3.2: Mechatronic design of the SEA brake pedal and the dynamometer

deflection [29, 30] that can be formed by crossing two leaf springs symmetrically. A cross-flexure pivot is preferred as the compliant element of the SEA, since this type of compliant pivot is robust as it distributes stress over the leaf springs, avoiding stress concentrations. The center of rotation of cross-flexure pivot is aligned with the rotation axis of the brake pedal (the ball bearing), while a Hall-effect sensor is constrained to move between the neodymium block magnets embedded in the sector pulley.

Figure 3.2 presents a solid model of the proposed system with design details. Deflection of the leaf springs is presented in Figure 3.3 [27]. Note that given that SEA brake pedal is designed to be attached to conventional friction brake pedal in parallel, the mechanical coupling between the brake pedal and friction brakes are maintained. Hence, even if the SEA brake pedal fails, it would be possible for the driver to stop the vehicle. SEA brake pedal may fail due to snapping of the capstan cable or electronics malfunction. In the former case, the driver will simply feel the friction brakes, while in the latter case the inertia and the friction of the DC motor/power transmission will be also reflected to the driver. Along these lines, the capstan transmission at the last level helps decrease friction forces and the geared motor needs to be selected to be passively backdriveable by the driver under emergency braking conditions.

3.2 Sensors and Power Electronics

SEA brake pedal necessitates (at least) two position sensors: one for measuring the rotations of the DC motor and another for measuring the deflections imposed on the elastic element. Since brake pedal is a safety critical element, sensor redundancy is preferred for enhanced safety. Along these lines, the DC motor is selected to include an optical encoder at its shaft.

A Hall-effect sensor embedded in the capstan measures the deflections of the compliant element. Furthermore, an optical encoder is also employed to measure deflections of the cross flexure joint to introduce sensor redundancy. Finally, the conventional friction brake pedals already have a displacement sensor which acts as a redundant sensor that can be used to detect any failure that may take place at the encoder on the DC motor presented in Figure 3.4.

The DC motor is driven by a PWM voltage amplifier, since the velocity (not the torque) of the motor is controlled by the fast inner motion control loop of cascaded control architecture of SEA (see Section 3.3) and any high frequency vibrations (possibly induced by PWM) are mechanically low-pass filtered by the compliant element before reaching to the driver.

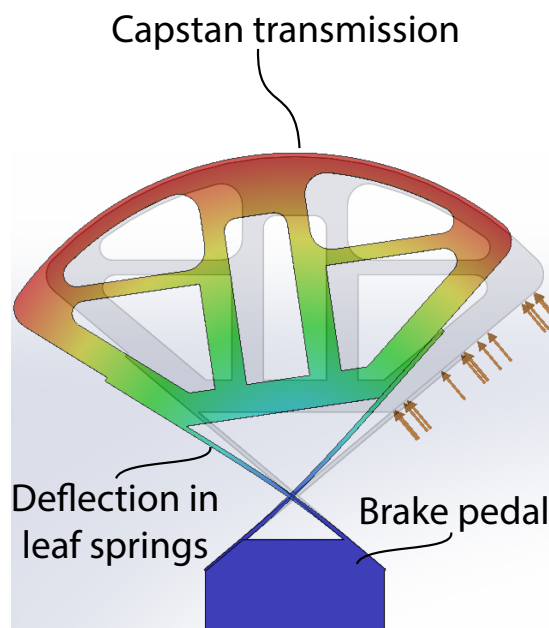


FIGURE 3.3: Deflection of leaf spring in cross-flexure joint

All sensors and the motor amplifier are connected to a real-time (EtherCAT) bus and the controllers are implemented on a microcontroller. The micro-controller is programmed through the Matlab/Simulink graphical interface and Embedded Coder toolbox, allowing for easy implementation of multi-rate control architectures with hard real-time performance. Note that similar development process is commonly used in the automotive industry and the control architecture is easily transferable to other bus and microcontroller architectures used in most vehicles.

3.3 Cascaded Loop Controller for SEA Brake Pedal

Cascaded controllers are implemented for the SEA brake pedal as shown in Figure 3.5. In this cascaded controller, the fast inner-loop running at 2.5 kHz controls the velocity of the geared motor, rendering it into an ideal motion source by compensating for imperfections in the power transmission, such as friction and stiction in the gearbox. The outer-loop, implemented at 1 kHz, controls the interaction torque based on the deflection feedback from the compliant element. The coupled stability of the cascaded control architecture of SEA is guaranteed within the frequency domain passivity framework with the proper choice of controller gains, as detailed in [7].

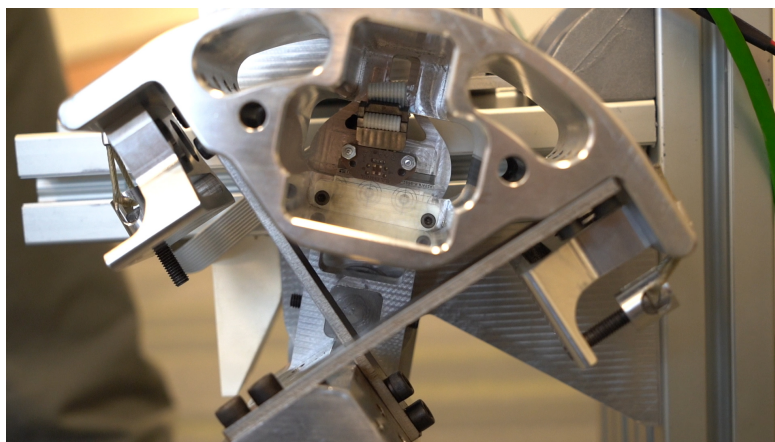


FIGURE 3.4: Measuring the deflection of cross-flexure joint by linear encoder

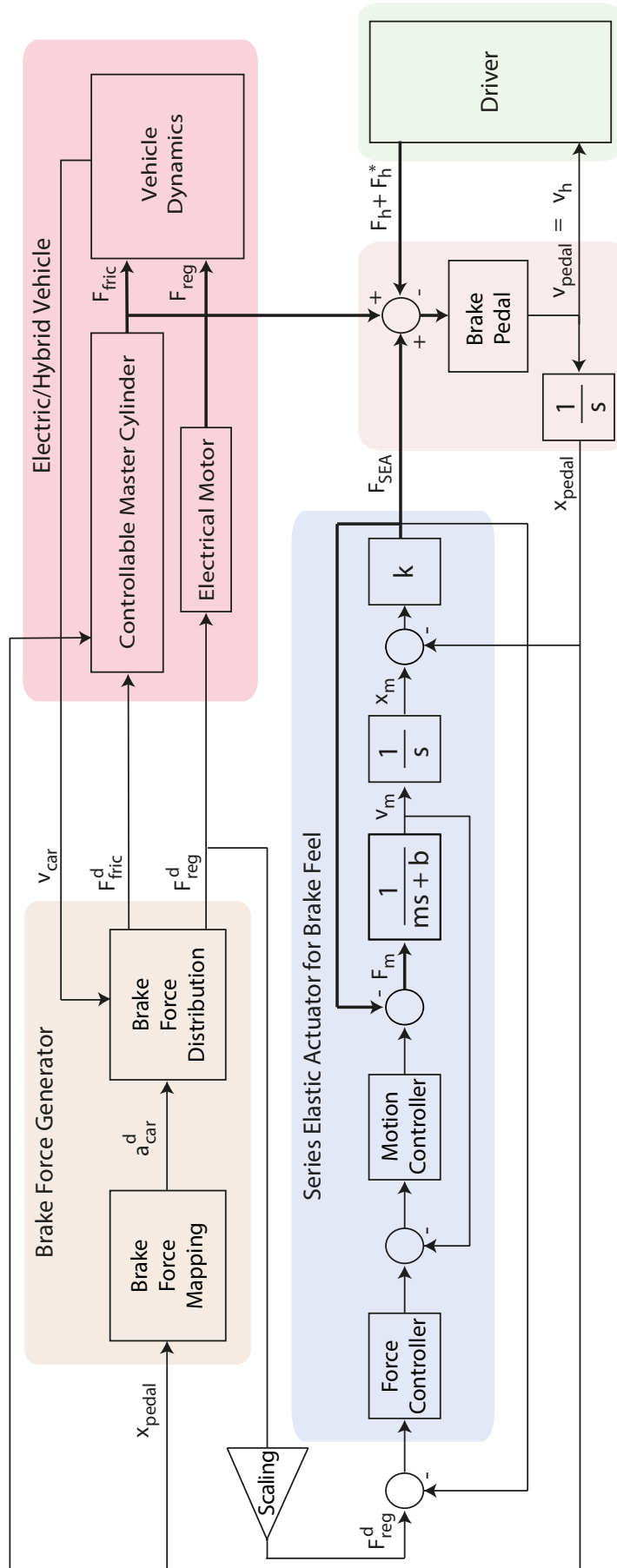


FIGURE 3.5: Block diagram of SEA brake pedal

Chapter 4

Design and Control of Haptic Pedal Feel Rendering Platform

In this chapter, the mechanical and control design of haptic pedal feel platform are presented.

4.1 Mechanical Design of Haptic Pedal Feel Rendering Platform

Figure 4.1 presents a solid model of the haptic pedal feel rendering platform developed for testing different regenerative braking approaches. The system consists of a SEA brake pedal and a torque controlled dynamometer that share identical designs, as depicted in Figure 3.2. The two force feedback devices are mechanically coupled to each other through a rigid connection. The dynamometer is used to render (electro)hydraulic friction brake reaction forces originating from the vehicle's controllable master cylinder, as well as other forces/disturbances acting on the brake pedal, while the force-feedback pedal is used to implement two-pedal cooperative braking and one-pedal driving to compensate for the disturbance effects and to recover the natural brake pedal feel.

4.1.1 Throttle Pedal

To enable simulation of one-pedal driving, an open-loop impedance controlled throttle pedal is included in the system, as presented in Figure 4.3. The throttle pedal consists of a direct drive motor with a 10:1 ratio capstan transmission such that forces up to 75 N can be provided the driver's foot. The throttle pedal position is utilized for determining the activation instant of the regenerative braking under one-pedal driving.

4.2 Control of the Haptic Pedal Feel Rendering Platform

Figure 4.2 presents the block diagram used to control the haptic pedal feel rendering platform. In the figure, the thick lines denote power coupling and the thin lines represent signals. Symbols m and b denote the effective inertia and damping of the identical SEA devices. Human applied forces are indicated by two distinct components: F_h representing the passive component and F_h^* denoting the intentionally applied active component, which are assumed to be independent of the

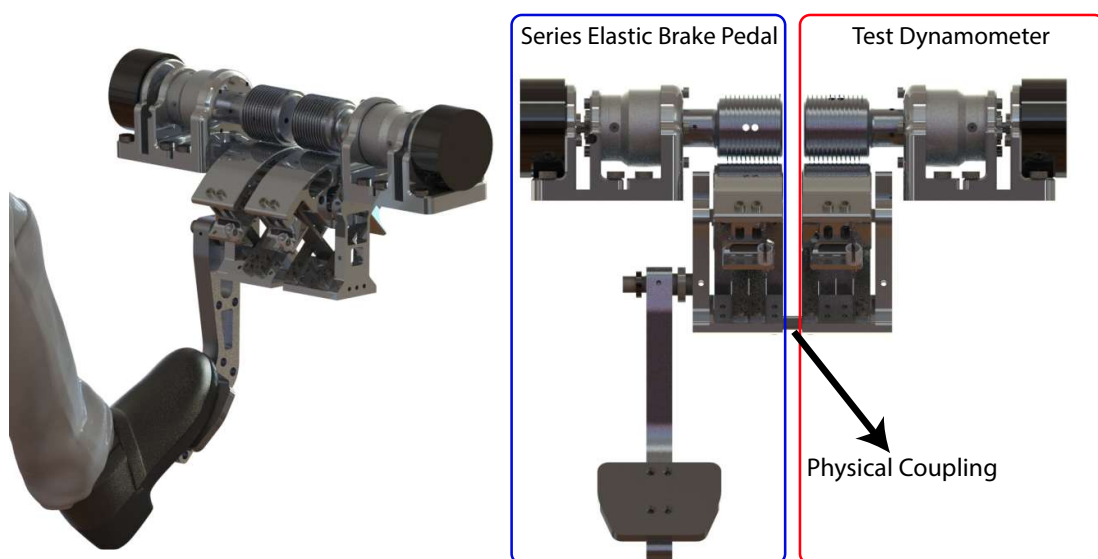


FIGURE 4.1: Regenerative brake development platform consists of a force-feedback brake pedal and a torque controlled test dynamometer

system states, such that coupled stability can be concluded through the frequency domain passivity framework [31].

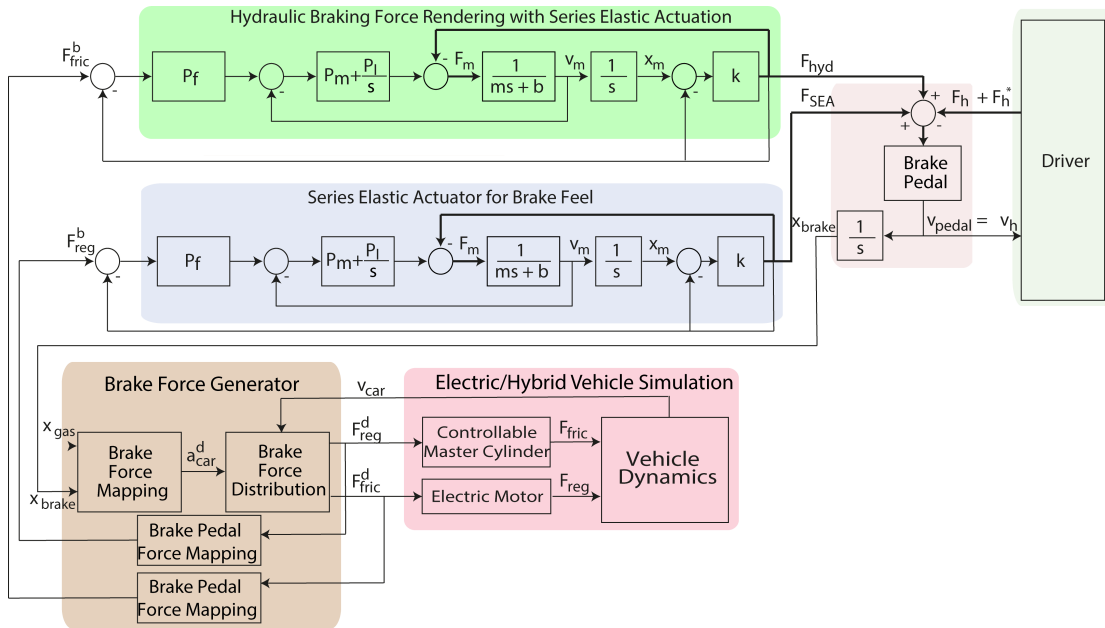


FIGURE 4.2: Control block diagram of haptic pedal feel rendering platform

In Figure 4.2, after appropriate mapping, the regenerative brake force demand F_{reg}^d is passed to the SEA brake pedal as a reference force. The SEA pedal relies on closed-loop force control to ensure that this reference force is rendered to the driver with high fidelity. Similarly, the friction force brake demand F_{fric}^d is passed to the dynamometer as a reference force such that (electro)hydraulic friction brake reaction forces originating from the vehicle's controllable master cylinder are rendered to the driver. Consequently, the driver feels the force-feedback from the total braking force applied to the vehicle, that is, the sum of forces from the friction brakes F_{hyd} through the dynamometer and forces from the regenerative brakes F_{SEA} through the SEA brake pedal.

The force/torque control of the brake pedal and the dynamometry are implemented as independent control loops, such that they can be run at different control rates and in an unsynchronized manner to be able to render more realistic disturbance and compensation forces. Independent real-time cascaded PI controllers are implemented for the control of series elastic actuators. Overall, the prototype of haptic pedal feel platform is depicted in Figure 4.3.

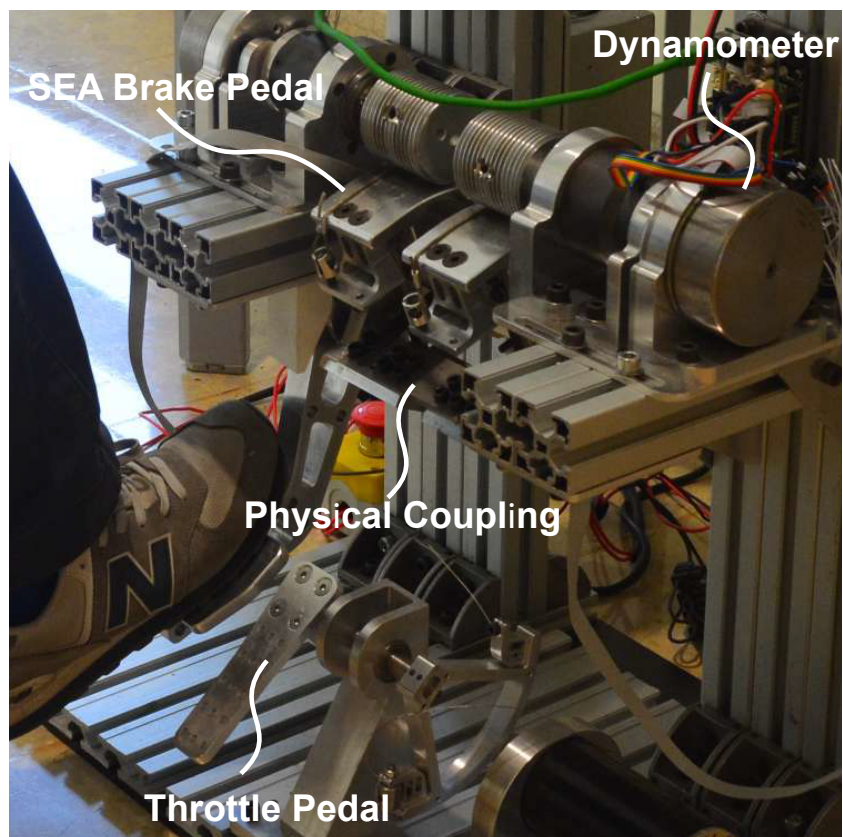


FIGURE 4.3: Haptic pedal feel rendering platform for cooperative braking

Chapter 5

Experimental Characterization of SEA Brake Pedal

In this chapter, the performance of the SEA brake pedal has been investigated. Inner controller parameters are determined by closed-loop system identification. The bandwidth of the inner loop is evaluated by fitting a first-order transfer function on the experimental data. Low, medium and high force control bandwidths are experimentally determined. The response of chirp and step inputs are presented.

5.1 System Identification

SEA brake pedal parameters are determined with closed-loop system identification. The system identification is performed with position control depicted in Figure 5.1. Closed-loop system identification is preferred because it can compensate for nonlinear effects (e.g., friction, stiction) in the mechanical system resulting in a linear system that is easier to identify.

The system is excited with eleven sinusoidal inputs with different frequencies. The frequency ranges from 0.1 Hz up to 18 Hz . The output position is measured with the integrated sensor of the motor. F_{SEA} is defined as the exogenous input to the system. During closed-loop system identification $F_{SEA} = 0$ because the

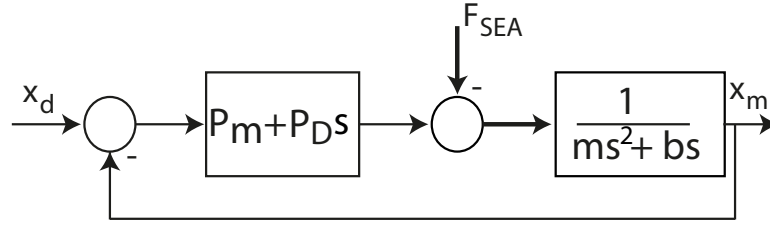


FIGURE 5.1: Closed-loop system used for identification of the SEA brake pedal

end-effector is free to move. Along these lines, the estimated transfer function is presented in in Eqn. (5.1).

$$H = \frac{P_D s + P_m}{J s^2 + (P_D + b) s + P_m} \quad (5.1)$$

In the closed-loop system identification procedure, System Identification Toolbox of MATLAB is used. The estimated transfer function system is depicted in Eqn. (5.2). From Eqn. (5.1), we can easily extract system's reflected inertia J and reflected damping B on the motor side. Estimated inertia, damping and controller gains are shown in Table 5.1.

$$H_{est} = \frac{0.06376 s + 2.541}{0.00064 s^2 + 0.08065 s + 2.541} \quad (5.2)$$

Figure 5.2 presents a validation for the closed-loop system identification. In particular, second order transfer function is fitted the experimental data. The estimated transfer function and the experimental data have a good match with an R^2 of 92%. From the transfer function, the cut-off frequency of the inner loop is can be determined as 19 Hz. Note that, PD control in position level corresponds to PI control in velocity level.

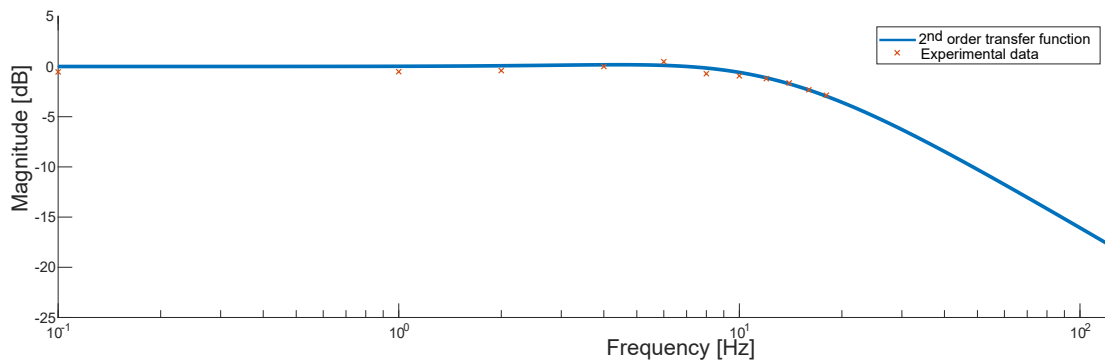


FIGURE 5.2: Experimental system identification of the SEA brake pedal

5.2 Force Bandwidth

To maximize the force control bandwidth, controller gains should be selected as high as possible. In cascaded control, the inner-loop acts as an ideal motion source within the motion control bandwidth. A perfect motion source rejects the disturbances to perfectly track the input motions. The outer-loop controller gain P_f should be maximized for high fidelity force rendering and robust control. Force control bandwidth is evaluated commonly for low, medium and high force amplitudes. To determine the force bandwidth of the system, the end-effector of the pedal is rigidly attached to the ground. Thus, end-effector velocity is set to zero. For estimating the force bandwidth of the system, the system is excited with a linearly increasing chirp input. For which the frequency range is between 0.1 Hz and 12 Hz .

In Figure 5.3, the low force control bandwidth is presented for input force magnitude of 5 Nm . Low force bandwidth is higher than 12 Hz . Medium force control

TABLE 5.1: SEA brake pedal plant parameters and controller gains

| Symbol | Description | Value | Unit |
|--------|-------------------------------------|--------|-----------|
| J | Plant inertia | 6399 | gcm^2 |
| B | Plant damping | 0.0169 | Nms/rad |
| P_m | Motion controller proportional gain | 0.0638 | Nms/rad |
| I_m | Motion controller integral gain | 2.541 | Nm/rad |
| P_f | Force controller propotional gain | 25 | rad/Nms |
| K | Cross-flexure joint stiffness | 362 | Nm/rad |

bandwidth is depicted in Figure 5.3 for input force magnitude of 10 *Nm* as 8.5 *Hz*. In Figure 5.3 high force control bandwidth for 15 *Nm* is indicated as 6 *Hz*.

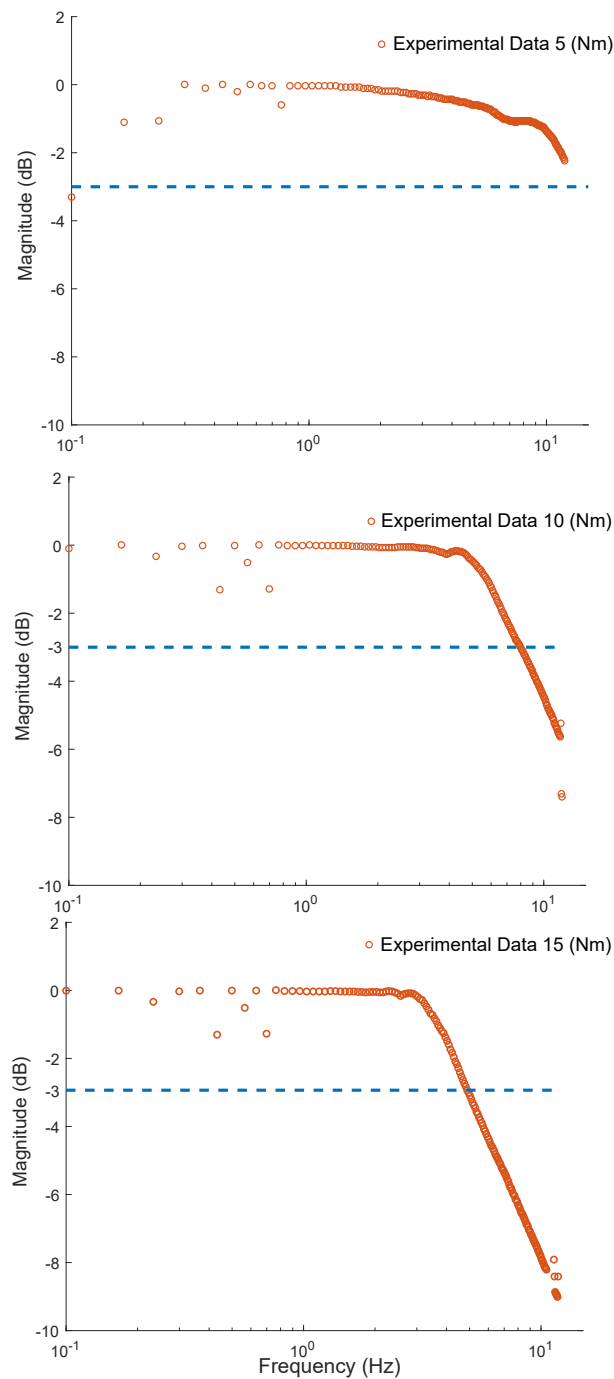


FIGURE 5.3: Low force (5 Nm) bandwidth, medium force (10 Nm) bandwidth, high force (15 Nm) bandwidth

5.3 Force Tracking Performance

In this section, the force tracking performance of the SEA brake pedal system is analysed. Figure 5.4 presents the response. A step response as a torque command is the input to the SEA brake pedal controller. The overshoot is less than 1% and the rise time is less than 50 *ms*. Response to a chirp input is presented in Figure 5.5, where the overshoot is less than 2%. Overall, the SEA brake pedal has a good torque tracking performance with in its bandwidth. The SEA brake pedal response time is an order of magnitude faster than the response time of a conventional brake booster [32].

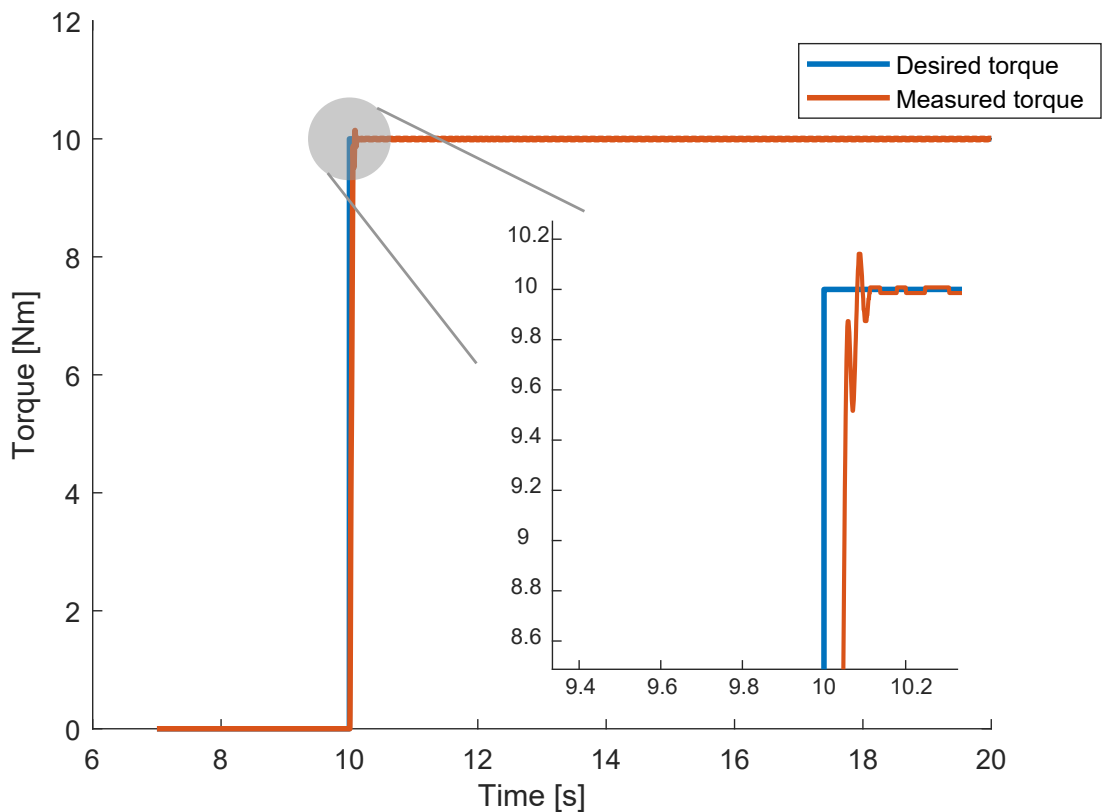


FIGURE 5.4: Step input force tracking performance in 10 [Nm]

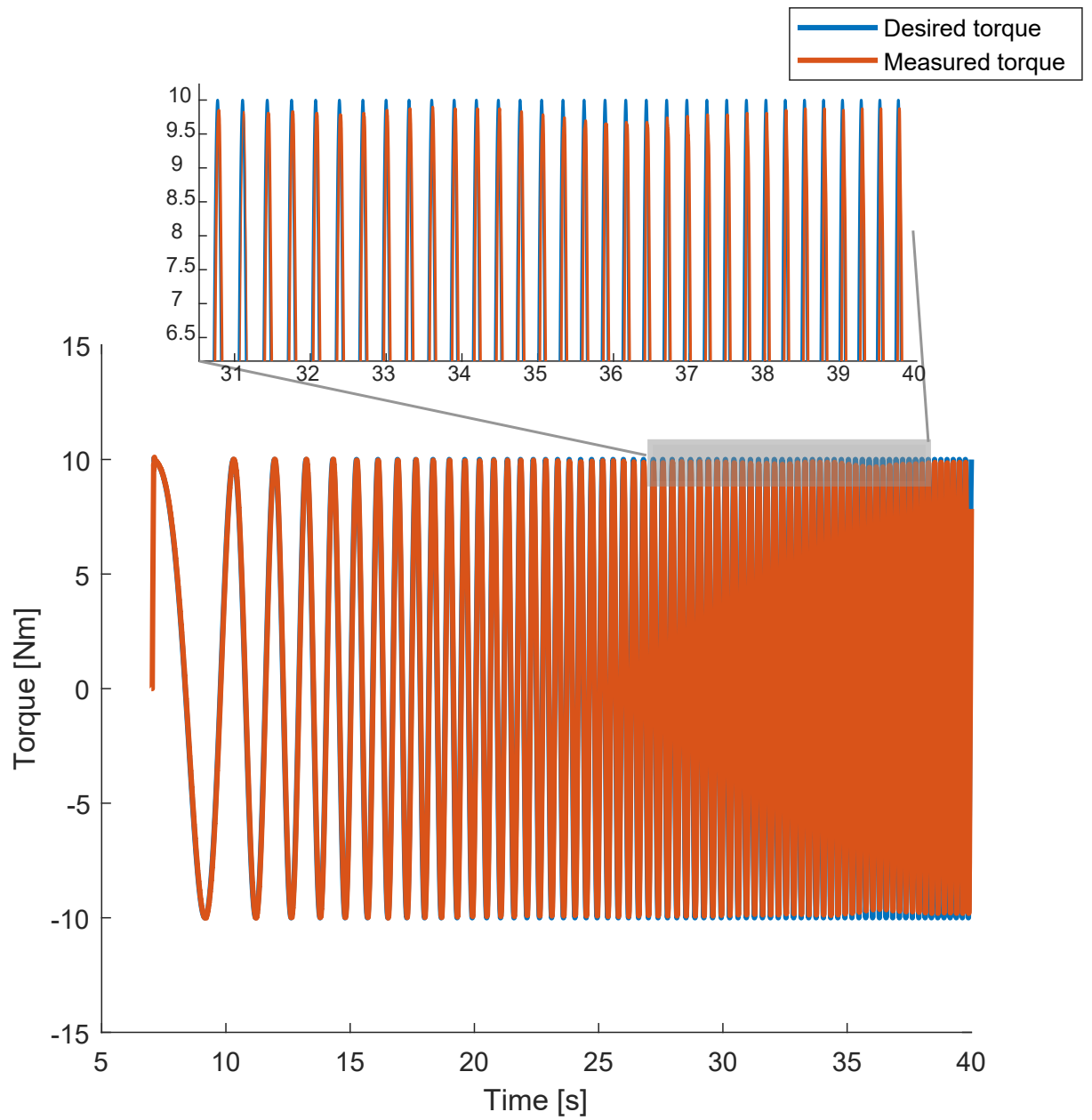


FIGURE 5.5: Chirp input force tracking performance in 10 [Nm]

Chapter 6

Haptic Pedal Feel Compensation Algorithms

In this section, pedal feeling rendering algorithms for two-pedal cooperative braking and one-pedal driving are detailed. In Figure 6.1, control of haptic pedal feel rendering platform is presented. *Brake Force Generator* block diagram distributes the brake force demand between regenerative braking and friction braking on the vehicle. Also, brake pedal force mapping is included in the *Brake Force Generator* block diagram which is detailed in Section 6.2. After appropriate mapping, the regenerative brake force demand F_{reg}^d is fed into the SEA brake pedal as a reference force. The friction force brake demand F_{fric}^d is passed into the dynamometer. Note that, dynamometer represents the hydraulic brake force originated from the controllable master cylinder. The dynamometer and SEA brake pedal have identical designs, such that the sum of forces from friction brakes F_{hyd} and the regenerative brake forces F_{SEA} are fed into the driver. Overall, the driver feels the total force applied to the vehicle through the SEA brake pedal and the dynamometer.

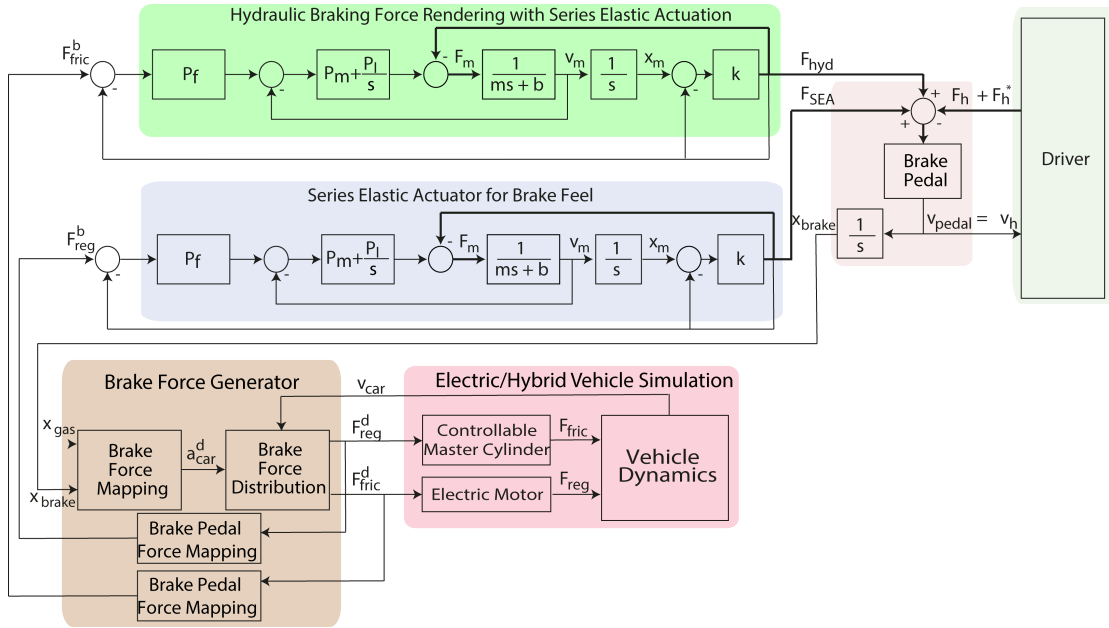


FIGURE 6.1: Control block diagram of haptic pedal feel rendering platform

6.1 Conventional Haptic Brake Pedal Feel

The conventional haptic brake pedal feel to be recovered is based on the brake booster model presented in [33]. In this model, brake booster reaction forces to the pedal is imitated with two distinct zones: the first zone capturing the vacuum valve spring stiffness and the second zone representing the air valve spring stiffness. The conventional pedal feel is mathematically modelled as

$$F_{pedal} [N] = \begin{cases} 0.80 x_{pedal} + 18.17 & x_{pedal} \leq 20\text{mm} \\ 3.92 x_{pedal} - 40.23 & 20\text{mm} < x_{pedal} \leq 80\text{mm} \end{cases} \quad (6.1)$$

where x_{pedal} denotes the pedal displacement with a maximum stroke of 80 mm and F_{pedal} is the total pedal force [34].

6.2 Brake Force Generator

Brake force generator block determines the brake force distribution in the vehicle. The pedal mapping and vehicle braking forces are modelled as follows.

6.2.1 Brake Pedal Displacement to Deceleration Mapping

For both driving conditions, the brake pedal displacement x_{pedal} is mapped to the deceleration demand a_{car}^d through the *Brake Force Mapping* block as

$$a_{car}^d \left[\frac{m}{sec^2} \right] = \begin{cases} -(0.01 x_{pedal})g & x_{pedal} \leq 20\text{mm} \\ -(0.02 x_{pedal} - 0.2)g & 20\text{mm} \leq x_{pedal} \leq 80\text{mm} \end{cases} \quad (6.2)$$

according to [34], where g represents the gravitational acceleration. The total demanded braking force F_{tot} is mapped from the deceleration demand a_{car}^d through the vehicle mass M_{car} .

6.2.2 Brake Force Distribution

Brake force distribution is decided based on the deceleration demand a_{car}^d from the driver, the instantaneous vehicle speed v_{car} , the battery charge level and the road conditions. A mathematical model of instantaneous regenerative braking force is employed as

$$F_{reg}^d [\text{N}] = \begin{cases} 0 & v_{car} \leq 4\text{m/s} \vee v_{car} \geq 33\text{m/s} \\ \frac{P_m}{v_{car}} & 4\text{m/s} < v_{car} \leq 33\text{m/s} \wedge (x_{brake} > 0 \vee x_{gas} = 0) \end{cases} \quad (6.3)$$

where $P_m = 15$ kW denotes the constant braking power of the electric motor [5]. Note that regenerative braking forces F_{reg}^d cannot be generated below/above some critical speed, in particular, below 4 m/sec (15 km/h) and above 33 m/sec (120 km/h) in this model. To avoid sudden changes in regenerative braking force, linear interpolation is used around the critical speeds to smooth out the transition.

Given the regenerative braking capacity at any instant and neglecting the road conditions for simplicity, the brake force distribution block determines the amount of regenerative and friction braking that needs to be employed, based on the one-pedal versus the two-pedal condition. In two-pedal cooperative braking the regenerative brake is activated when the brake pedal is pressed, while in one-pedal driving the regenerative brake is activated when the throttle pedal is released.

In two-pedal cooperative braking, the friction brake force is decided based on the available regenerative braking force as F_{Fric}^d [N] = $F_{tot} - F_{reg}^d$. In one-pedal driving, by pressing the (emergency) brake pedal, only the friction brake is activated; hence, the pedal displacement to force mapping is direct and based solely on F_{Fric} .

6.2.3 Brake Pedal Force Mapping

One-pedal driving and two-pedal cooperative braking have identical pedal force mappings. Both the regenerative braking force F_{reg}^d and the friction brake force F_{fric}^d are mapped to the pedal force as

$$F_{pedal}^b$$
 [N] =
$$\begin{cases} 0.0333 F_{brake}^d - 40.21 & F_{brake}^d \geq 2352 \text{ N} \\ 0.0085 F_{brake}^d + 18.17 & 0 \text{ N} \leq F_{brake}^d < 2352 \text{ N} \end{cases} \quad (6.4)$$

where $F_{brake}^d = \{F_{reg}^d, F_{fric}^d\}$. In no compensation cases, F_{reg}^d is set to zero, as pedal forces for regenerative braking are not rendered.

6.3 Two-pedal Cooperative Braking and One-pedal Driving Simulations

In Figures 6.2 and 6.3, sample cooperative braking scenarios with and without haptic brake pedal feel compensation are presented for two-pedal and one-pedal driving respectively. In the first row of the figures, the velocity of the vehicle is depicted, while the pedal displacement is presented in the second row. For the one-pedal driving case, the throttle displacement is also presented. In the third row, the regenerative braking forces, friction brake forces and total brake forces are depicted. The last row presents the pedal forces felt by the driver. In these sample scenarios, pedals are assumed to be displaced in a linear manner, for the simplicity of presentation. The results are under the assumption of perfect force tracking within the SEA devices bandwidth.

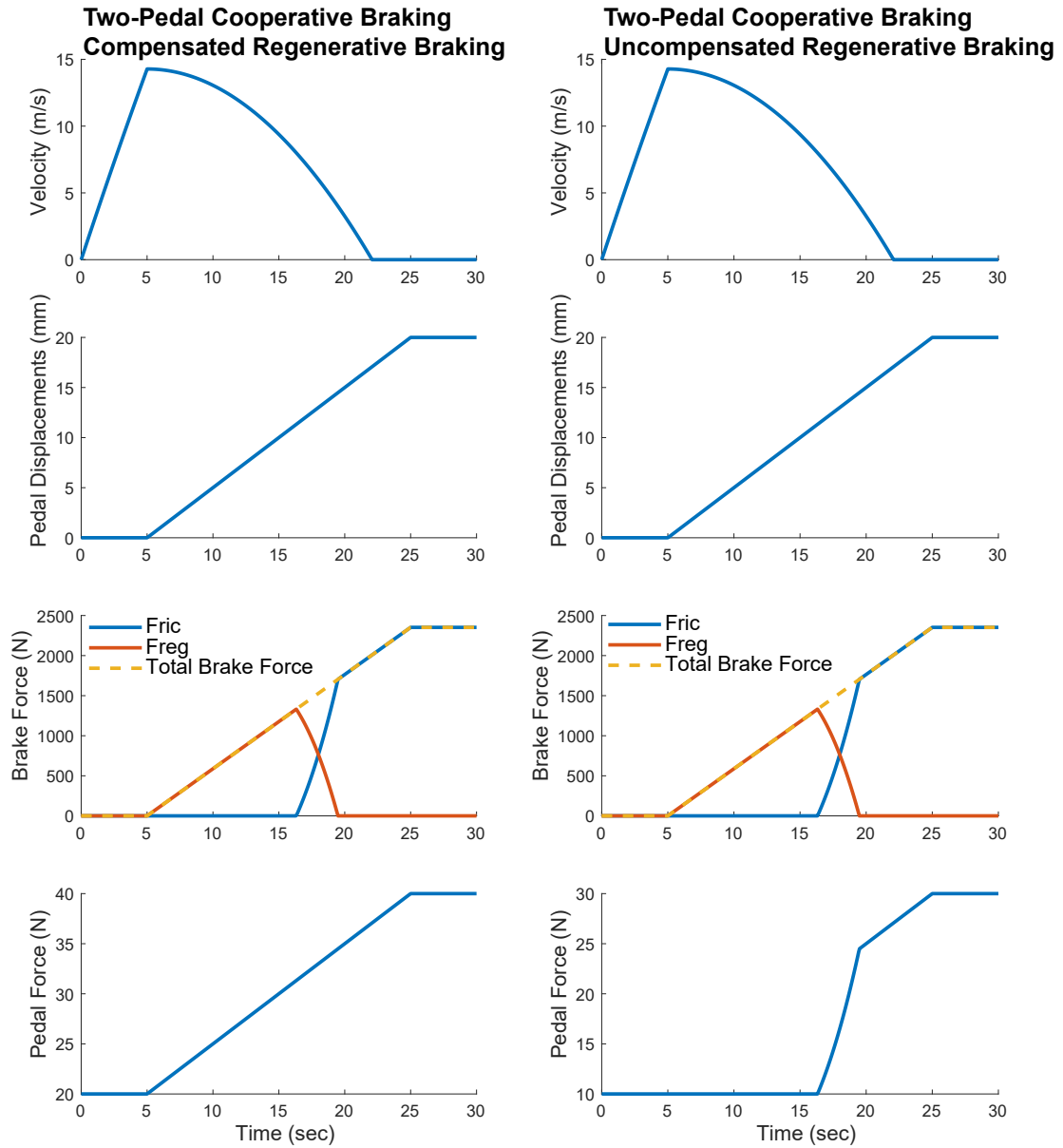


FIGURE 6.2: A sample scenario for two-pedal cooperative braking with and without haptic pedal feel compensation

In Figures 6.2 and 6.3, all four conditions are implemented using the block diagram in Figure 3.5 with different *Brake Force Generation* maps as detailed in Section 6.2. In these sample scenarios, pedal is assumed to be displaced in a linear manner, as this input allows for clear presentation of the differences between compensated and uncompensated cases, under one-pedal driving and two-pedal cooperative braking.

6.3.1 Two-Pedal Cooperative Braking

In two-pedal cooperative braking, regenerative brake is activated by pressing the brake pedal. When there is a deceleration demand from the driver, the regenerative braking is utilized as much as possible. When the deceleration demand is higher than that can be supplied by the regenerative braking, the friction brake is activated. In the uncompensated case, there exists no pedal force due to regenerative braking, while in the compensated case, relevant pedal forces are rendered to the pedal as discussed in previous subsection.

In Figure 6.2, when the driver presses the brake pedal at $t = 5$ s, regenerative brake is employed to the maximum capacity. The regenerative braking forces increase in a nonlinear fashion, as the vehicle slows down. Note that no pedal force exists for the non-compensated case when friction brake is not in use. Since the regenerative braking forces cannot be generated at velocities lower than 4 m/sec, the friction brake is employed at $t = 16$ s such that the desired deceleration demand can be delivered. Starting this instant, brake pedal forces go through a sharp increase in the uncompensated condition until the friction brake takes over the whole braking at $t = 20$ s. After $t = 20$ s, the uncompensated pedal feels like a conventional friction brake. Note that the compensation eliminates the discontinuities and stiffening/softening of haptic pedal feel due to regenerative braking and delivers a continuous conventional brake pedal forces throughout the cooperative braking.

6.3.2 One-Pedal Driving

One-pedal driving and two-pedal cooperative braking differ in that regenerative braking is activated when the throttle pedal is released in one-pedal driving. In particular, when the driver releases the throttle pedal, the maximum available regenerative braking force is utilized until a threshold (chosen as 0.32g in this study) after which the force is saturated not to induce an uncomfortable deceleration level. If the driver presses the emergency brake pedal, further use of regenerative braking may be activated as in cooperative braking, while typically the friction brake is

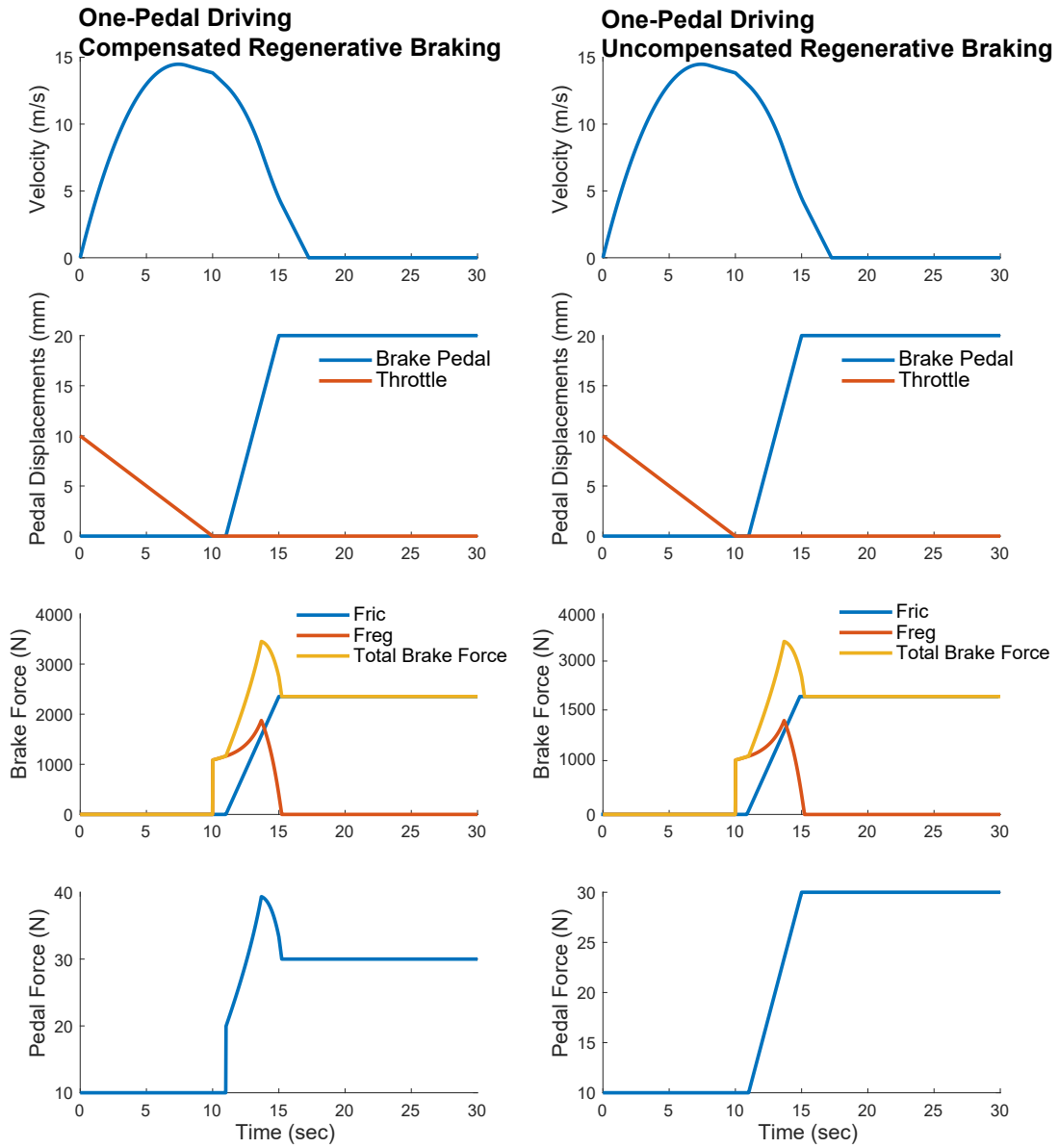


FIGURE 6.3: A sample scenario for one-pedal driving with and without haptic pedal feel compensation

activated, as most capacity of regenerative braking is already in use. In the uncompensated case, there exists no pedal force due to regenerative braking, while in the compensated case, relevant pedal forces are rendered to the emergency brake pedal to achieve a linear relationship with the total braking force.

In Figure 6.3, the driver releases the throttle pedal at $t = 10$ s, which activates the regenerative braking, but does not render any forces to the emergency brake pedal in both cases, as it is not being pushed yet. The displacement of the emergency brake pedal is increased linearly during $t = 11$ – 15 s and the friction brake is

activated, as the deceleration from regenerative braking is not sufficient to provide the demanded deceleration. In the uncompensated case, the driver feels only the reaction forces from the friction brake. While this force is continuous, the mapping between the pedal force and the total brake force is nonlinear. In the compensated case, this mapping is linear.

Chapter 7

User Evaluations

In this chapter, we evaluate the efficacy of the SEA brake pedal via a haptic pedal feel platform. One-pedal driving and two-pedal cooperative braking algorithms are implemented on the haptic pedal feel platform. Compensated and uncompensated conditions investigated on one-pedal and two-pedal driving separately. These four distinct conditions are evaluated in terms of safety, performance and energy efficiency.

7.1 Participants

Ten volunteers (8 males and 2 female) with ages between 22 to 28 participated in the experiment. All participants had active driver's licenses and none of them had any prior experience with vehicles equipped with regenerative braking. All participants signed an informed consent approved by the IRB of Sabanci University.

7.2 Driving Simulator

The simulator setup consisted of an SEA brake pedal, a dynamometer, a throttle pedal and a vehicle simulator, as presented in Figure 7.1. Participants were seated in a vehicle seat and adjusted the seat position according to their preferred driving

position. The simulator provided visual feedback through two flat screens displays. The front screen displayed the simulated vehicle pursuit scenario, while the left monitor showed the vehicle speed.

7.3 Task

We tested the usefulness and efficacy of pedal feel compensation through SEA brake pedal during cooperative regenerative braking in a braking simulator. The braking simulator is based on a simplified version of the Crash Avoidance Metrics Partnership (CAMP) protocol [35]. The simulation takes place on virtual straight road of 1500 m, where the controlled vehicle follows a leading vehicle. The leading vehicle accelerates at 0.2 g until it reaches the target speed of 50 km/h. Once it reaches 50 km/h the leading vehicle decelerates until stop, and then after waiting for a short random interval, it re-accelerates back to 50 km/h. In particular, the leading vehicle decelerates with 0.19 g, 0.28 g and 0.39 g at random instances within the 0-500 m, 500 m-1000 m, and 1000 m-1500 m stretches of the road. The leading vehicle stops permanently at the end of the road. Initially, the following vehicle is placed 15 m behind the leading vehicle.

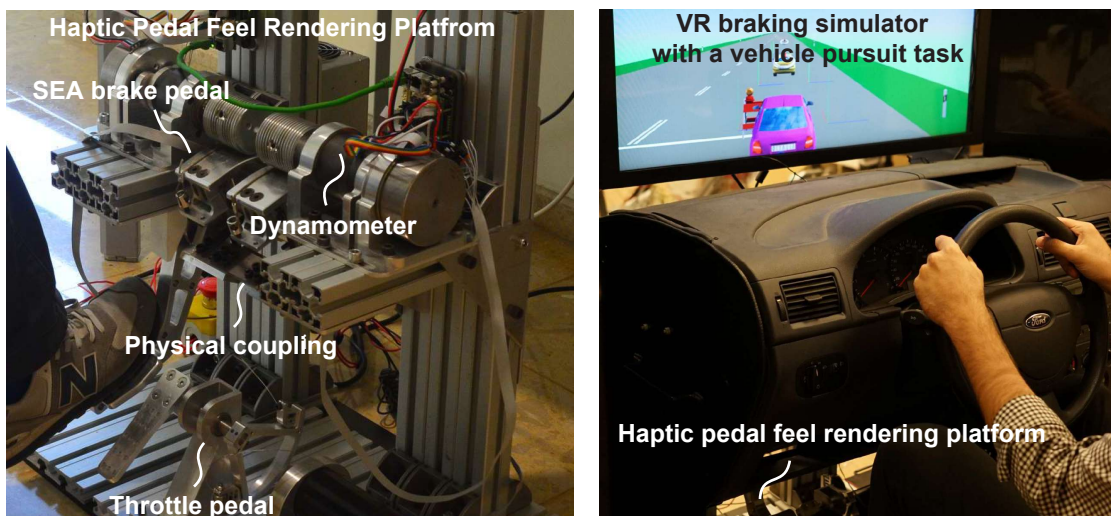


FIGURE 7.1: Cooperative braking simulator

This vehicle also accelerates automatically at 0.2 g until it reaches the target speed of 50 km/h, if the brake pedal is not pressed, while the participants can decelerate the car by pressing the SEA brake pedal to control the distance to the leading vehicle.

7.4 Experimental Procedure

Effect of two main factors of compensation and pedal type are investigated. In particular the within subjects experiment protocol involved *two-pedal uncompensated*, *two-pedal compensated*, *one-pedal uncompensated* and *one-pedal compensated* conditions tested on the same volunteers. At the beginning of experiments an unrecorded session was implemented, during which all four conditions were displayed to the volunteers in a randomized order to help them familiarize with the braking simulator. Then, volunteers were assigned to test conditions in a randomized order. The volunteers were informed about one pedal versus two pedal driving condition, but not about the existence/lack of compensation. After each trial, they were asked to recognize the existence of compensation.

7.5 Performance Metrics

Several quantitative metrics are defined to evaluate the driving performance of the participants. The number of times *hard brakings* were necessitated during the trials is selected as a safety performance metric, as large decelerations are potentially dangerous. Decelerations over 0.5g are considered as hard braking [35]. For pursuit tracking performance analysis, the distance between two vehicles is selected as the performance metric and % *RMSE* is calculated with respect to the instructed distance of 30 m. To evaluate the efficiency of driving, regenerated energy is calculated by adding the regenerative power at each time step over the trial duration T as $E_{reg} = \mu \int_0^T F_{reg} v_{car} dt$, where $\mu = 0.8$ denotes the efficiency of energy recovery. Furthermore, percent throttle use is also computed.

Finally, the volunteers are asked to fill in a short questionnaire to help evaluate their qualitative preferences among the test conditions. The questionnaire included nine questions as presented in Table 7.1. A 5-point Likert scale is used to indicate preferences, where 5 denotes strong agreement and 1 denotes strong disagreement.

7.6 Analysis

A two-way repeated measures ANOVA is conducted to determine the significant effects on the quantitative metrics. The within-within factors are taken as compensation (compensated/uncompensated) and pedal type (two-pedal/one-pedal). Box plots of important metrics are present to enable multi-comparisons and effect size evaluations.

7.7 Experiment Results

In this section, second set of experiments have been presented. In this experiment set, two-pedal driving condition and one-pedal driving condition have been investigated in terms of *driving performance*, *safety*, *energy efficiency*, and *survey*.

7.7.1 Safety

Figure 7.2 presents the box plot for the number of hard brakings. Two-way repeated measures ANOVA indicates that the interaction of compensation and pedal type factors is significant with $F(1,9) = 9.51$, $p = 0.014$. The compensation is significant, while the pedal type is not significant at the $p < 0.05$ level.

For the simple main effect analysis, the data is first split for two-pedal and one-pedal driving conditions. For the two-pedal driving condition, hard brakings in the compensated case ($M = 1.2$, $SD = 0.33$) are significantly lower than the uncompensated case ($M = 4.4$, $SD = 0.56$) with $F(1,9) = 39.05$, $p < 0.001$.

The effect size is significant as the number of hard brakings have increased more than 3.5 times in the uncompensated case. Similarly, for the one-pedal driving condition, hard brakings in the compensated case ($M = 1.8$, $SD = 0.36$) are significantly lower than the uncompensated case ($M = 2.8$, $SD = 0.53$) with $F(1, 9) = 5.63$, $p = 0.042$. The effect size is also significant as the number of hard brakings has increased by 55% in the uncompensated case.

The data is also split for compensated and uncompensated conditions. For the uncompensated condition, hard brakings instances in the two-pedal condition ($M = 4.4$, $SD = 0.56$) are significantly higher than the one-pedal case ($M = 2.8$, $SD = 0.53$) with $F(1, 9) = 5.43$, $p = 0.045$. The effect size is significant as the number of hard brakings has increased more than 57% in the two-pedal case. For the compensated group, pedal type is not a significant factor at the $p < 0.05$ level.

7.7.2 Pursuit Tracking Performance

Two-way repeated measures ANOVA indicates that compensation, pedal type, and interaction are not significant factors for the % *RMSE* metric quantifying the tracking performance at the $p < 0.05$ level.

7.7.3 Energy Efficiency

Figure 7.3 presents the box plot for the percent throttle use. Two-way repeated measures ANOVA indicates that one-pedal driving ($M = 40.1$, $SD = 3.1$) results in significantly higher throttle use compared to two-pedal cooperative braking ($M = 25.86$, $SD = 4.25$) with $F(1, 9) = 6.92$, $p = 0.034$. Compensation and interaction are not significant at the $p < 0.05$ level. The effect size is significant as the throttle use has increased by 60% in the one-pedal driving case.

Figure 7.4 presents the box plot for the regenerated braking energy. One-pedal driving ($M = 3.096$, $SD = 0.25$) results in significantly higher regenerated

TABLE 7.1: Survey Questions and Summary Statistics

| Cronbach $\alpha > 0.96$ | Mean | σ^2 |
|--|------|------------|
| Q1: Do you feel the intervention of friction brake under the two-pedal uncompensated regenerative brake condition? | 4.6 | 0.49 |
| Q2: Can you stop the car within the desired distance and time under the two-pedal uncompensated regenerative brake condition? | 3.2 | 0.60 |
| Q3: Do you feel the intervention of friction brake under the two-pedal compensated regenerative brake condition? | 1.4 | 0.49 |
| Q4: Can you stop the car within the desired distance and time under the two-pedal compensated regenerative brake condition? | 4.2 | 0.60 |
| Q5: Do you feel the intervention of friction brake under the one-pedal uncompensated regenerative brake condition? | 1.9 | 0.70 |
| Q6: Can you stop the car within the desired distance and time under the one-pedal uncompensated regenerative brake condition? | 3.0 | 0.63 |
| Q7: Do you feel the intervention of friction brake under the one-pedal compensated regenerative brake condition? | 2.1 | 0.70 |
| Q8: Can you stop the car within the desired distance and time under the one-pedal compensated regenerative brake condition? | 4.2 | 0.87 |
| Q9: Does the compensated brake pedal offer a conventional brake feel? | 4.3 | 0.64 |
| Frequency | | |
| Q10: Do you prefer the one-pedal driving or the two-pedal driving condition? | 50% | 50% |
| Q11: Do you prefer the compensated or the uncompensated regenerative braking condition? | 90% | 10% |

energy compared to two-pedal cooperative braking ($M = 1.035$, $SD = 0.045$) with $F(1, 9) = 70.15$, $p < 0.001$, while compensation and interaction are not significant at the $p < 0.05$ level. The effect size is significant as 3 times more energy is regenerated during the one-pedal driving.

7.7.4 Qualitative Metrics

Survey questions together with their summary statistics are presented in Table 7.1. The Cronbach's α for the questionnaire is evaluated to be greater than 0.96, indicating a high reliability of the survey.

Q1 measured the level of intervention of friction brake under the uncompensated regenerative brake condition and participants *strongly agreed* that they were able to feel the intervention.

Q2 quantified if the participants were able to stop the car under the uncompensated regenerative brake condition and the participants *agreed* that they could stop the car within the desired distance and time.

Q3 measured the level of intervention of friction brake under the compensated regenerative brake condition and participants *strongly disagreed* that they were able to feel the intervention.

Q4 quantified if the participants were able to stop the car under the compensated regenerative brake condition and the participants *highly agreed* that they could stop the car within the desired distance and time.

Q5 measured the level of intervention of friction brake under the one-pedal uncompensated condition and participants *strongly disagreed* that they were able to feel the intervention.

Q6 quantified if the participants were able to stop the car under the one-pedal uncompensated condition and the participants *agreed* that they could stop the car within the desired distance and time.

Q7 measured the level of intervention of friction brake under the one-pedal compensated regenerative brake condition and participants *highly disagreed* that they were able to feel the intervention.

Q8 quantified if the participants were able to stop the car under the one-pedal compensated condition and the participants *highly agreed* that they could stop the car within the desired distance and time.

Q9 measured if the compensated brake pedal was similar to a conventional brake feel, and the participants *highly agreed* that the feel of the pedal was similar to a conventional one.

Q10 asked participants which experiment condition they preferred; 5 of the participants preferred the one-pedal condition, while 5 of them preferred the two-pedal condition.

Q11 asked participants which experiment condition they preferred; 9 of the participants preferred the compensated condition, while 1 of them preferred the uncompensated condition.

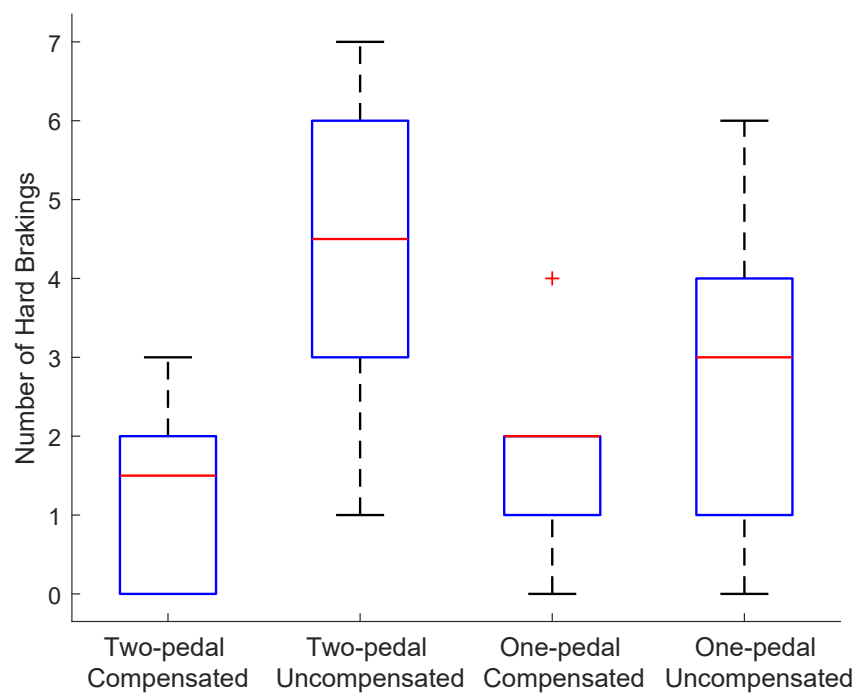


FIGURE 7.2: Box plot of number of hard brakings

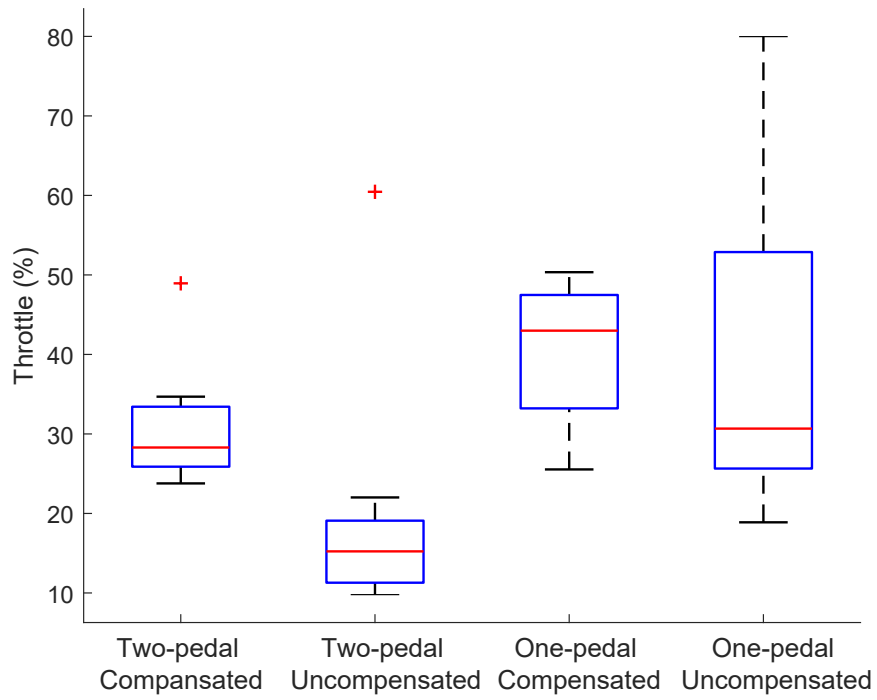


FIGURE 7.3: Box plot of percent throttle use

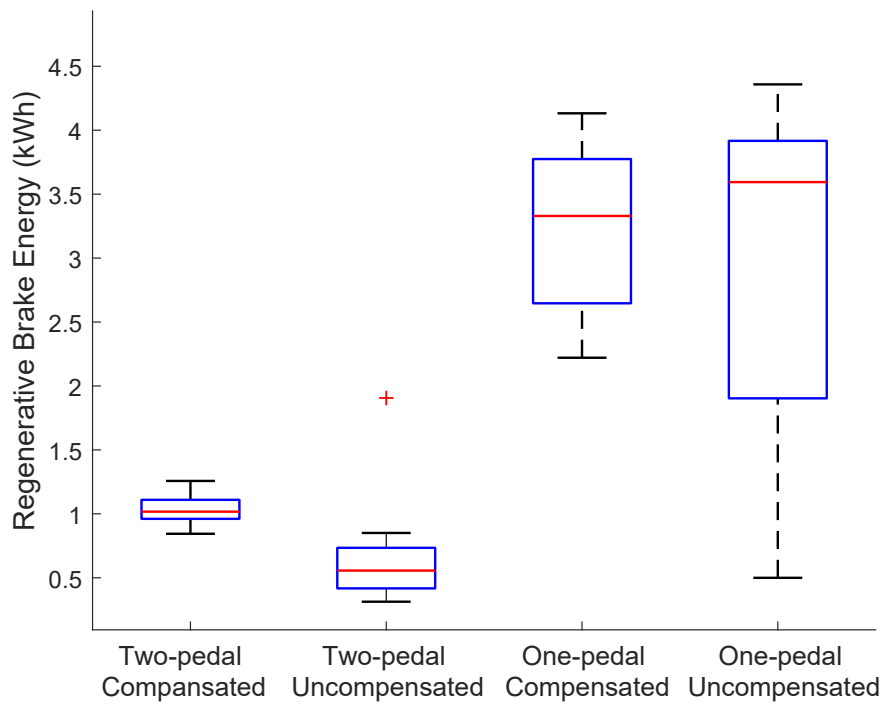


FIGURE 7.4: Box plot of regenerative braking energy

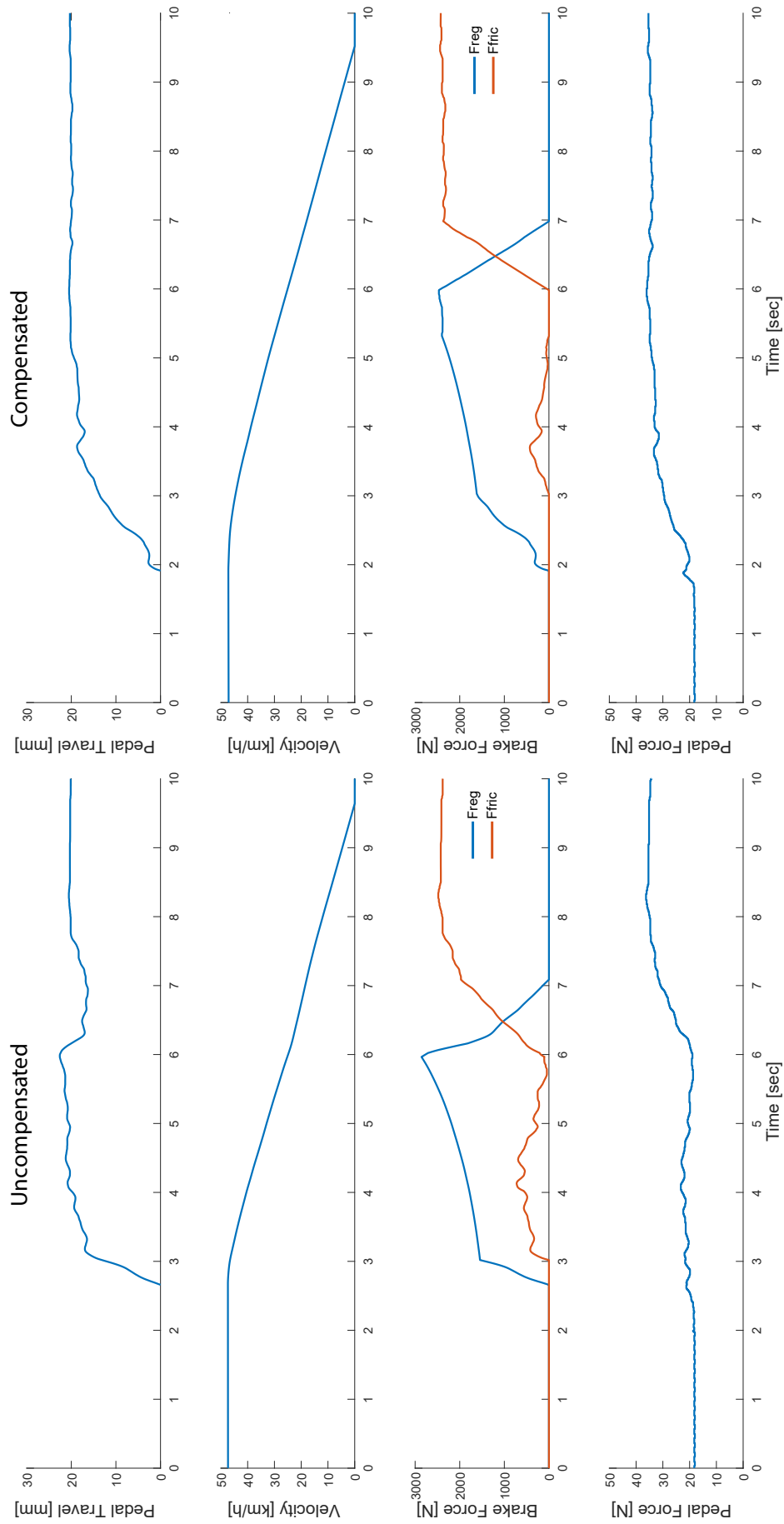


FIGURE 7.5: Sample experimental results collected under uncompensated and compensated conditions

Chapter 8

Discussion of User Studies

To evaluate the performance of 4 conditions 3 qualitative metrics have been defined as safety, tracking performance and energy efficiency. These metric are widely used in automotive industry to have better safety and experience while driving.

Safety is one the key aspect for evaluating the driving performance. The number of hard brakings is a commonly used safety metric, as it is important for the drivers to be able to predict the stopping distance and safely decelerate the vehicle accordingly. The addition of regenerative braking results in a nonintuitive brake pedal force to deceleration mapping that significantly reduces the driver performance in terms of the need for hard brakings. Given that the regenerative braking is highly nonlinear and strongly affected by the instantaneous state of the vehicle, long training periods may be necessary for drivers to adjust to this nonintuitive brake mapping. Compensation of haptic pedal feel recovers the natural brake pedal feel by removing the nonlinearities and the strong dependence to the instantaneous state. In the compensated case, there exists a linear mapping between the pedal force and the total braking force that results in a significant decrease in the need for hard brakings, for both one and two pedal driving conditions.

In terms of the number of hard brakings, compensation has a larger positive effect for the two-pedal cooperative braking. While in the compensated case, both

one pedal and two-pedal case have similar performance, the performance of two-pedal cooperative braking is significantly worse for the uncompensated case, as the brake pedal stays very soft during the regenerative braking phase of two-pedal cooperative braking and then suddenly stiffens, causing the drivers to overshoot the proper pedal position. On the other hand, drivers mostly experience the reaction forces from the friction brake during one-pedal driving, which results in a relatively more predictable pedal behaviour, even though the deceleration mapping is still nonlinear.

In two-pedal cooperative braking to better study the change in brake feel, a follow-up experiment was conducted. In these trials, the goal of the participants were to press the pedal and keep the pedal displacement at a constant level near 20 mm to decelerate the vehicle from 50 km/h to halt. The vehicle speed and pedal displacement feedback were displayed to the participants on the monitor to assist them with the task. Figure 7.5 presents sample experimental data collected under the two experimental conditions, to better illustrate the differences in the pedal feel under compensated and uncompensated conditions. From these plots, one can observe that the participants had hard time keeping the pedal position constant under the intervention of friction braking when the compensation was off. This intervention is best observed around $t = 6$ s, where the regenerative braking could no longer generate forces and friction brakes were employed to compensate for the lack of regenerative braking. All participants were able to keep the pedal position constant with minimal effort for the compensated case.

According to the survey results, the volunteers strongly agree that compensated brake pedal offers a conventional brake feel and there is a significant intervention in the two-pedal uncompensated braking condition, while they strongly disagree with the existence of intervention in the compensated case. The volunteers also disagree that one-pedal compensated and uncompensated conditions have intervention. This result is also attributed to the relatively more predictable pedal forces in the uncompensated one-pedal driving case.

Consequently, for safe driving, compensated regenerative braking conditions is strongly preferred by 90% of the volunteers and quantitatively advantageous, especially in two-pedal cooperative braking. The beneficial effect of compensation is comparatively smaller in one pedal driving, while the difference is still statistically significant and existence of compensation results in substantial quantitative effect size in terms of the number of hard brakings. Hence, haptic pedal feel compensation is highly recommended for both driving conditions to enable more predictable decelerations of the vehicle.

In terms of the pursuit tracking performance, the volunteers were able to adequately adjust the distance between two vehicles in all conditions with no significant differences. In the survey, the volunteers agree that they can stop the car within the desired distance in both compensated conditions, while they are neutral to both uncompensated conditions. However, hard brakings negatively affect driving, as sharp decelerations are disturbing. Consequently, for the driving performance, compensated regenerative braking conditions are both more strongly preferred and advantageous.

In terms of the throttle use, one pedal driving necessitates significantly more use of the accelerator, as the use of throttle is required even for coasting. In terms of the total regenerated brake energy, one-pedal driving results in a significantly higher regeneration level, since regenerative brakes are more frequently used, as this type of brake engages as soon as the driver releases the throttle pedal. The compensation does not have a significant effect on throttle use or the total regenerated brake energy, as the need for cooperative braking is quite infrequent compared to throttle use and mild regenerative braking during the simulated pursuit tracking task.

While one-pedal driving recovers significantly more energy from regeneration, this does not necessarily imply better energy efficiency of the vehicle, as it also results in significantly more throttle use. Proper evaluation of the overall energy efficiency requires further investigation, as a more detailed dynamic model of the

vehicle and efficiency of the power electronics during acceleration and regeneration need to be considered, along with a more comprehensive highway/city driving task.

For simulating the conventional brake feel, two-zone stiffness is added in this study for mimicking the brake booster effect presented in [34],[33]. In the future, the brake booster is eliminated by the brake-by-wire systems. Eliminating the brake booster may lead to a single zone stiffness. Since the SEA brake pedal's brake force mapping is adjustable, it is suitable for brake-by-wire systems and current vehicles with different architectures.

Test dynamometer and the gas pedal are added into braking simulator. Also, a vehicle simulator is used during experiments. Test dynamometer is a hydraulic braking simulator which is physically coupled to the SEA brake pedal. In a control perspective, it is acting as a disturbance for the SEA brake pedal. Thanks to SEA's nature with aggressive gains, SEA brake pedal can compensate for the disturbing effects. Table 7.1 indicates that the participants are feeling little or no discontinuity or abrupt pedal forces during the experiments. Also, the participants are agreed in two-pedal compensated regenerative braking condition is similar to conventional pedal feel.

Chapter 9

Conclusion

In conclusion, a series elastic brake pedal has been implemented and its efficacy in recovering the conventional smooth brake pedal feel during two-pedal cooperative braking and one-pedal driving has been demonstrated. Haptic pedal feel platform is proposed and it consists of the dynamometer, the gas pedal and the SEA brake pedal to evaluate the regenerative braking algorithms. Compensation of haptic pedal feel has been shown to be advantageous, especially in terms of safety and driver preferences, for both two-pedal cooperative braking and one-pedal driving. While the volunteers equally prefer and can effectively utilize both two-pedal and one-pedal driving conditions. The beneficial effects of haptic pedal feel compensation on safety is evaluated to be larger for the two-pedal cooperative braking condition, as lack of compensation results in stiffening/softening pedal feel characteristics in this case.

Future works include the integration of the proposed series elastic brake pedal in a physical vehicle with regenerative braking capabilities and conducting larger-scale human subject experiments on more realistic scenarios. Two-pedal cooperative braking and one-pedal driving should be investigated with a more advanced model of the vehicle for maximizing energy efficiency during driving.

Bibliography

- [1] S. A. Oleksowicz, K. J. Burnham, A. Southgate, C. McCoy, G. Waite, G. Hardwick, C. Harrington, and R. McMurrin, “Regenerative braking strategies, vehicle safety and stability control systems: Critical use-case proposals,” *Vehicle System Dynamics*, vol. 51, no. 5, pp. 684—699, 2013.
- [2] F. Wang and B. Zhuo, “Regenerative braking strategy for hybrid electric vehicles based on regenerative torque optimization control,” *Proc. of the Institution of Mechanical Engineers, Part D: Journal of Automobile Engineering*, vol. 222, no. 4, pp. 499–513, 2008.
- [3] J. Zhang, C. Lv, J. Gou, and D. Kong, “Cooperative control of regenerative braking and hydraulic braking of an electrified passenger car,” *Proc. of the Institution of Mechanical Engineers, Part D: Journal of Automobile Engineering*, vol. 226, no. 10, pp. 1289–1302, 2012.
- [4] N. Ohkubo, S. Matsushita, M. Ueno, K. Akamine, and K. Hatano, “Application of electric servo brake system to plug-in hybrid vehicle,” *SAE Int. J. Passeng. Cars – Electron. Electr. Syst.*, vol. 6, no. 1, 2013.
- [5] C. N. Kumar and S. C. Subramanian, “Cooperative control of regenerative braking and friction braking for a hybrid electric vehicle,” *Proc. of the Institution of Mechanical Engineers, Part D: Journal of Automobile Engineering*, vol. 230, no. 1, pp. 103–116, 2015.
- [6] R. D. Howard, *Joint and actuator design for enhanced stability in robotic force control*. PhD thesis, Massachusetts Institute of Technology, 1990.

-
- [7] F. E. Tosun and V. Patoglu, “Necessary and sufficient conditions for passivity of velocity-sourced impedance control of series elastic actuators,” *CoRR*, vol. abs/1902.10607, 2019.
- [8] D. Lindvai-Soos and M. Horn, “Modelling, control and implementation of an electro-mechanic braking force actuator for HEV and EV,” *IFAC Proceedings Volumes*, vol. 46, no. 21, pp. 620–625, 2013.
- [9] S. Stachowski, K. Pavlov, and R. Stevenson, “Motor driven feedback mechanism,” 2004.
- [10] H. de Rosario, M. Louredo, I. Diaz, A. Soler, J. J. Gil, J. S. Solaz, and J. Jornet, “Efficacy and feeling of a vibrotactile frontal collision warning implemented in a haptic pedal,” *Transportation Research Part F: Traffic Psychology and Behaviour*, vol. 13, no. 2, pp. 80–91, 2010.
- [11] J. van Boekel, I. Besselink, and H. Nijmeijer, “Design and realization of a one-pedal-driving algorithm for the tu/e lupol,” *World Electric Vehicle Journal*, vol. 7, pp. 227–237, 2015.
- [12] Y. Saito and P. Raksincharoensak, “Effect of risk-predictive haptic guidance in one-pedal driving mode,” *Cognition, Technology and Work*, vol. 21, pp. 671–684, 2019.
- [13] R. Nilsson, “Evaluation of a combined brake–accelerator pedal,” *Accident Analysis and Prevention*, vol. 34, no. 2, pp. 175–183, 2002.
- [14] H. H. Wen, W. Chen, and J. Hui, “A single-pedal regenerative braking control strategy of accelerator pedal for electric vehicles based on adaptive fuzzy control algorithm,” *Energy Procedia*, vol. 152, pp. 624–629, 2018.
- [15] L. Yu, X. Liu, Z. Xie, and Y. Yi Chen, “Review of brake by wire system used in modern passenger,” in *ASME International Design Engineering Technical Conferences and Computers and Information in Engineering Conference*, 2016.

-
- [16] J. W. Zehnder, S. S. Kanetkar, and C. A. Osterday, “Variable rate pedal feel emulator designs for a brake-by-wire system,” Tech. Rep. 1999-01-0481, Delphi Automotive Systems Chassis Systems, January 1999.
- [17] Y. Randolph and D. Agnew, “Brake pedal feel simulator,” 2008.
- [18] I. Jung, J. Jeon, and J. Lee, “Magneto rheological brake pedal simulator,” 2005.
- [19] Z. Tan, Z. Chen, X. Pei, and J. Zhang, “Research and simulation of electro hydraulic braking system based on integrated master cylinder,” in *SAE World Congress and Exhibition*, 2015.
- [20] H. Vollert and J. Mayer, “Electromechanical brake booster,” 2014.
- [21] M. IFlad, S. Rothfuss, G. Diehm, and Hohmann.S, “Active brake pedal feedback simulator based on electric drive,” *SAE International Journal of Passenger Cars*, pp. 189–200, 2014.
- [22] D. Crombez and D. Gabor, “Automotive braking system with master cylinder force simulator,” 2010.
- [23] W. S. P. Abeyesiriwardhana and A. H. S. Abeykoon, “Simulation of brake by wire system with dynamic force control,” in *IEEE International Conference on Information and Automation for Sustainability*, 2014.
- [24] M. Mulder, *Haptic Gas Pedal Feedback for Active Car-Following Support*. PhD thesis, Technische Universiteit Delft, 2007.
- [25] J. W. Sensinger and R. F. f. Weir, “Unconstrained impedance control using a compact series elastic actuator,” in *IEEE/ASME International Conference on Mechatronics and Embedded Systems and Applications*, 2006.
- [26] S. Eppinger and W. Seering, “Understanding bandwidth limitations in robot force control,” in *IEEE International Conference on Robotics and Automation*, vol. 4, pp. 904–909, 1987.

-
- [27] A. Otaran, O. Tokatli, and V. Patoglu, “Hands-on learning with a series elastic educational robot,” in *Haptics: Perception, Devices, Control, and Applications*, pp. 3–16, Springer International Publishing, 2016.
- [28] G. Pratt and M. Williamson, “Series elastic actuators,” in *IEEE/RSJ International Conference on Intelligent Robots and Systems*, vol. 1, pp. 399–406, 1995.
- [29] B. D. Jensen and L. L. Howell, “The modeling of cross-axis flexural pivots,” *Mechanisms and Machine Theory*, vol. 37, pp. 461–476, 2002.
- [30] Z. Hongzhe and B. Shusheng, “Stiffness and stress characteristics of the generalized cross spring pivot,” *Mechanisms and Machine Theory*, vol. 45, pp. 378–391, 2010.
- [31] J. E. Colgate and N. Hogan, “Robust control of dynamically interacting systems,” *Int. Journal of Control*, vol. 48, no. 1, pp. 65–88, 1988.
- [32] S. L and K. S-L, “Characterization and development of the ideal pedal force, pedal travel, and response time in the brake system for the translation of the voice of the customer to engineering specifications,” *Proceedings of the Institution of Mechanical Engineers Part D Journal of Automobile Engineering*, vol. 224, pp. 1433–1450, 11 2010.
- [33] A. J. Day, H. P. Ho, K. Hussain, and A. Johnstone, “Brake system simulation to predict brake pedal feel in a passenger car,” in *SAE 2009 Brake Colloquium and Exhibition*, 2009.
- [34] A. Spadoni, *Adaptive Brake By Wire From Human Factors to Adaptive Implementation*. PhD thesis, Univ. of Trento, 2013.
- [35] J. D. Hoffman, J. D. Lee, T. L. Brown, and D. V. McGehee, “Comparison of driver braking responses in a high-fidelity simulator and on a test track,” *Journal of the Transportation Research Board*, vol. 1803, no. 1, pp. 59–65, 2014.